The regulation of RHEB subcellular localisation

in early zebrafish myofibres

Zur Erlangung des akademischen Grades eines

DOKTORS DER NATURWISSENSCHAFTEN

(Dr. rer. nat.)

von der KIT-Fakultät für Chemie und Biowissenschaften

des Karlsruher Instituts für Technologie (KIT)

genehmigte

DISSERTATION

von

Raphael Fettig

1. Referent/Referentin: Prof. Dr. Andrew Cato

2. Referent/Referentin: Prof. Dr. Martin Bastmeyer

Tag der mündlichen Prüfung: 06.02.2024

Erklärung zur Urheberschaft

Hiermit erkläre ich, diese Dissertation selbstständig verfasst und keine anderen als die angegebenen Hilfsmittel verwendet zu haben. Wörtliches oder indirekt übernommenes Gedankengut ist nach bestem Wissen als solches gekennzeichnet worden. Dies ist mein erster Dissertationsversuch, ich habe keine erfolglosen Dissertationsversuche unternommen. Die Dissertation wurde bisher zu keinem Zeitpunkt als Prüfarbeit verwendet oder als Dissertation bei einer anderen Fakultät vorgelegt.

_____

Raphael Fettig

I Zusammenfassung

Der Signalweg „mechanistic target of rapamycin complex 1“ (mTORC1) ist eine treibende Kraft des Skelettmuskulaturwachstums, dies wird durch die Förderung der Hypertrophie der Muskelzellen, Muskelfasern genannt, erzielt. Verschiedene Signalwege konvergieren, um im Zytosol den direkt vorgeschalteten Aktivator von mTORC1, die kleine GTPase RHEB, zu aktivieren. RHEB ist durch seine C-terminale Farnesylierung an Endomembranen verankert, insbesondere an der des Lysosoms. Darüber hinaus kann RHEB auch im Zellkern vorhanden sein, zum Beispiel im Zellkern embryonaler Muskelfasern von Zebrabärblingen. Dort fördert RHEB unabhängig von mTORC1 das Muskelwachstum. In adulten Zebrabärblingen ist RHEB jedoch vorwiegend im Zytosol vorhanden. Dies weist auf eine Regulierung der subzellulären Lokalisation von RHEB während der Entwicklung hin. In dieser Arbeit habe ich zunächst die zeitliche Koordinierung der Zellkernlokalisation von RHEB in den embryonalen Muskelfasern von Zebrabärblingen untersucht. Ich konnte zeigen, dass RHEB vor dem Schlüpfen, in den embryonalen Stadien, im Zellkern lokalisiert ist. Diese Präsenz im Zellkern nahm nach dem Schlüpfen nach und nach ab. Da das Schlüpfen mit einem Anstieg der Muskelaktivität verbunden ist, habe ich den Effekt von Muskelkontraktion auf die Zellkernlokalisation von RHEB untersucht. Das Reduzieren der Muskelaktivität führte zu einer verlängerten Zellkernlokalisation von RHEB, das Erhöhen zu einer beschleunigten Reduktion. Vor dem Hintergrund der fördernden Wirkung von Muskelkontraktion auf die Muskelfaserreifung wäre es möglich, dass die skizzierten Erkenntnisse auf einen allgemeinen Prozess hinweisen, der in Verbindung mit Zellreifung zu einer Abnahme der Zellkernlokalisation von RHEB führt. Letztlich führte die Hemmung der Farnesylierung in den Muskelfasern geschlüpfter Zebrabärblingen zu einer Retention von nuklearem RHEB. Aufgrund dieser Ergebnisse nehme ich an, dass RHEB in unreifen Zellen in zwei Formen auftritt, einerseits farnesyliert und zytosolisch und andererseits unfarnesyliert und nuklear. Vollständige Zellreifung würde demnach zu einer vollständigen Farnesylierung von RHEB führen, welches vorwiegend im Zytosol vorhanden wäre. Dies deutet zudem darauf hin, dass nukleares RHEB bei der Zelldifferenzierung und der Zellreifung eine Rolle spielt.

II Abstract

The mechanistic target of rapamycin complex 1 (mTORC1) pathway is the main driver of skeletal muscle growth, by promoting the hypertrophy of skeletal muscle cells, the myofibres. Various signals converge to activate its direct upstream activator, the small GTPase RHEB in the cytosol. RHEB is anchored to endomembranes, in particular that of the lysosome, through its C-terminal farnesylation. Furthermore, RHEB can also be present in the nucleus, for example in the nucleus of zebrafish embryonic myofibres, where it promotes growth in an mTORC1-independent manner. However, RHEB is predominantly cytosolic in adult zebrafish myofibres, suggesting a regulation of RHEB subcellular localisation during development. In this work I first investigated the timing of RHEB nuclear localisation in embryonic zebrafish myofibres. I showed that RHEB is present in the nucleus at embryonic stages, before hatching. This presence in the nucleus then progressively decreased. Given that hatching is associated with an increased skeletal muscle activity, I then studied the effect of contraction on RHEB nuclear localisation. Reducing muscle activity in embryos prolonged the presence of RHEB in the nucleus, while increasing muscle activity accelerated the reduction of nuclear RHEB. This effect might be related to the maturation-promoting effect of contraction. This suggests that the decrease in RHEB nuclear localisation is a general process linked to maturation. Finally, inhibiting farnesylation resulted in the nuclear retention of RHEB in post-hatching myofibres. Based on these results, I assume that in immature cells RHEB exists as two pools, one farnesylated and cytosolic and the other non-farnesylated and nuclear. Upon final maturation, all RHEB would be farnesylated and predominantly retained in the cytosol. This also suggest a function for nuclear RHEB in cell differentiation and maturation.

III Index

IV Figure Index

V Abbreviations

BSA	Bovine serum albumin
dpf	Days post fertilization
FTI	Farnesyltransferase inhibitor
hpf	Hours post fertilization
LSM	Laser scanning confocal microscope
mRNA	Messenger RNA
mTORC1	mTOR complex 1
mTORC2	mTOR complex 2
NES	Nuclear export signal
NLS	Nuclear localisation signal
PBS -/-	Phosphate buffered saline without calcium or magnesium
Pol	Polymerase
PTU	Phenylthiourea
rRNA	Ribosomal RNA
TOS	TOR signaling motif

1. Introduction

1.1. Skeletal muscles

Skeletal muscles are an important tissue in the body, representing a major portion of total body mass. This proportion can vary in different vertebrates. In humans, skeletal muscles represent 30-40% of body mass (Janssen et al., 2000). In zebrafish they can exceed 50% of the total body mass, as the skeletal muscles continuously grow throughout their life (Mommsen, 2001). Skeletal muscles exert a multitude of functions, such as posture, mechanical force generation and locomotion. Furthermore, skeletal muscles contribute to the control of breathing and the regulation of the metabolism.

In mammals, muscles are made up of bundles of myofibres, which are their basic cellular unit (figure 1). The muscles are surrounded by layers of connective tissue. In zebrafish the body is segmented in distinct repeating muscle units along the anterior-posterior axis, arranged in a typical chevron shape (figure 1). These muscle units are known as myotomes and are surrounded by connective tissue. The myofibres are aligned in parallel in these myotomes (Kimmel et al., 1995; Waterman, 1969).

Myofibres are long, multinucleated cells. They are surrounded by the sarcolemma, a cell membrane, and contain thousands of parallel myofibrils. These myofibrils consist of long series of sarcomeres, which are the contractile unit of the muscle (figure 1). Sarcomeres, in turn, are formed of myofilaments. These chains of proteins, primarily actin and myosin, are arranged in specific characteristic patterns. These are further supported by proteins necessary for other mechanical and physiological properties (Frontera & Ochala, 2015). These myofilaments can move against each other in what is called the power stroke of the sarcomere. The power stroke is a contraction of the sarcomere and as the sarcomeres are synchronised this leads to the contraction of the myofibrils and thus the entire myofibre.

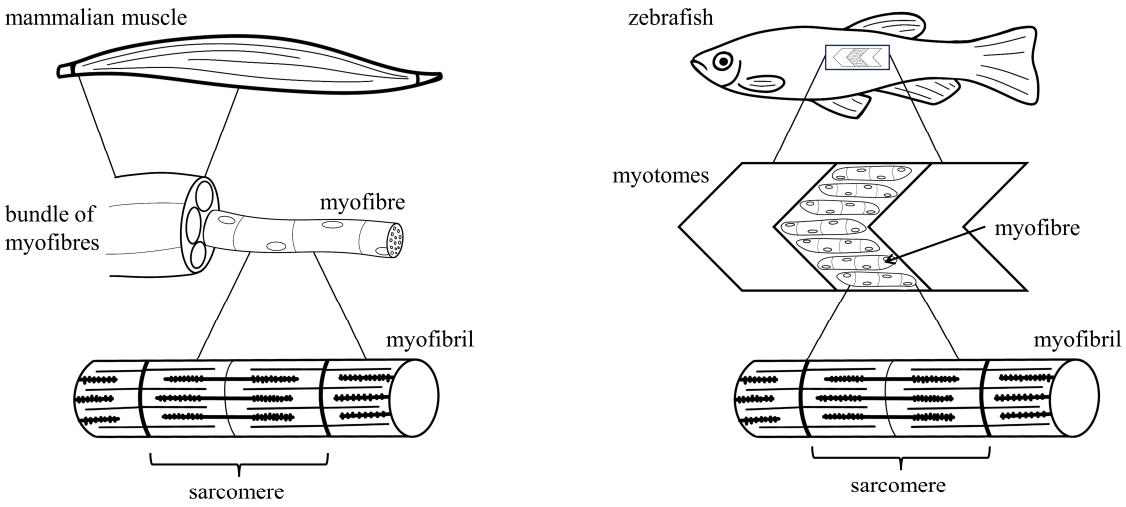

Figure 1: Schematic representation of mammalian and zebrafish muscles

Mammalian muscles are made of bundles of myofibres. These are comprised of thousands of myofibrils, which in turn are long repeating series of sarcomeres. In contrast zebrafish muscles are repeating muscle units called myotomes which are arranged in a chevron shape. In these myotomes the myofibres are parallel. Zebrafish myofibres are also made of myofibrils organized in sarcomeres.

Myofibres are formed in a process known as myogenesis. Progenitor cells first proliferate as mononucleated myoblasts. These exit the cell cycle and start differentiating into precursor cells, the myocytes. Myocytes in turn fuse to form multinucleated immature myofibres, the myotubes, which in turn mature into functional myofibres (Abmayr & Pavlath, 2012; Chal & Pourquié, 2017). Myogenesis can be categorized into embryonic and adult myogenesis. Embryonic myogenesis is essential for muscle formation, whereas adult myogenesis plays a key role in muscle repair and regeneration. In adult myogenesis quiescent muscle stem cells (satellite cells) located between the basal lamina and the sarcolemma (Yin et al., 2013) exit quiescence, proliferate and give rise to the myoblasts. While muscle size is pre-determined in mammals, zebrafish can continuously grow throughout their entire life (Mommsen, 2001). For embryonic myogenesis many events are common in all vertebrates, both in mammals and zebrafish (as a representative of the teleost). Among these are the regulation of progenitor cell fate, proliferation, differentiation and fusion, as well as the genetic regulation through transcription factors (Barresi et al.,

2001; Devoto et al., 1996; Devoto et al., 2006; Rescan, 2001). Despite this, there are several differences in both the timing and mechanisms of development.

In mammals, embryonic myogenesis occurs well into segmentation, involving muscle progenitor cells from the dermomyotome. In mice, segmentation and somitogenesis begins on embryonic day 8.5 (of 19 days of gestation) and ends on embryonic day 13 (Saga, 2012). The dermomyotome is an epithelial layer of proliferating precursor cells, which gives rise to the trunk, muscles and dermis (Hollway et al., 2007; Stellabotte et al., 2007; Stellabotte & Devoto, 2007). In mammals there are two regions of the dermomyotome. One gives rise to the deeper muscles of the back, the other to the more superficial muscles, as well as the diaphragm, the body wall and limb muscles (Cossu et al., 2000).

In zebrafish, there are two populations of muscle precursor cells. One is known as adaxial cells, which commit to embryonic myogenesis before segmentation (Devoto et al., 1996; Stickney et al., 2000). The other population, the lateral presomitic cells, only start differentiation after the onset of segmentation (Henry & Amacher, 2004). In zebrafish, somitogenesis occurs very early into development, starting at 10.3 hours post fertilization (hpf) and ending at 24 hpf, hatching occurring between 2 days post fertilization (dpf) and 3 dpf (Kimmel et al., 1995). Together, the adaxial and lateral presomitic cells form the primary myotome which is already functional after segmentation. In zebrafish the initial formation of the myotome is independent of the dermomyotome (Hollway et al., 2007; Stellabotte et al., 2007). Myogenic progenitor cells from the dermomyotome are however necessary for continued growth of the myotome (Devoto et al., 2006). The timepoint of the first muscle contraction and the onset of the heartbeat differs in mammals and zebrafish. Mice experience the first myocardial pulsation (heartbeat) on embryonic day 9 (Navaratnam et al., 1986), the first movement can be detected on embryonic day 12.5 (Suzue, 1996) and body movement begins on embryonic day 14 (Kodama & Sekiguchi, 1984). In Zebrafish the first muscle contractions in the form of random twitching can start occurring after 17 hpf, while the heartbeat starts at 24 hpf. The overall muscle activity is low until it starts increasing in preparation for hatching at 60 hpf, with free movement

occurring post hatching in the larval form (Kimmel et al., 1995; Saint-Amant & Drapeau, 1998).

Myofibres are very plastic cells, allowing skeletal muscles to adapt in structure and function as a response to a variety of stimuli. These stimuli include the presence and availability of nutrients and growth factors, as well as pathophysiological conditions and mechanical overload. This plasticity allows for the adaptation of various characteristics, such as their force-generation capacity, their resistance to fatigue, their ability to change contraction velocity, their repair capability, and their ability to change mass (Chromiak & Antonio, 2008; Flück & Hoppeler, 2003; Furrer et al., 2023).

1.2. Control of muscle size

In mammals, the mass of skeletal muscles is primarily determined by the size of the myofibres (Rennie et al., 2004). Therefore, changes to the overall muscle mass are primarily a result of changes in the size of pre-existing myofibres, as opposed to changes to the number of myofibres. Increasing the size of myofibres results in an increase in overall muscle mass, this is known as hypertrophy. Whereas a reduction in myofibre size results in a reduction in muscle mass, known as atrophy. In many fish, hyperplasia, an increase in the number of myofibres, is a further possibility for muscle growth (Mommsen, 2001). However, in zebrafish very little hyperplasia takes place after the juvenile phase has been reached (Biga & Goetz, 2006).

Individual myofibres, when excluding water content, are comprised of approximately 80% structural and functional protein (Frontera & Ochala, 2015). Thus, an important aspect of controlling myofibre size is the regulation of the available proteins. The degradation of proteins can lead to a reduction of myofibre size and ultimately to muscle atrophy, whereas increased protein synthesis can result in an increase in myofibre size and muscle hypertrophy. Therefore, the balance between the processes of protein synthesis and degradation plays an important role in determining the size of myofibres (Goldberg, 1969; Rennie et al., 2004). Environmental factors and various signalling pathways tightly

control these processes. They modulate gene expression at not only the transcriptional level but also the translational level. Furthermore, they can affect protein degradation and autophagy (Sandri, 2008).

1.3. The mechanistic target of rapamycin (mTOR)

The mTOR signalling pathway derives its name from the serine/threonine kinase mechanistic (formerly mammalian) target of rapamycin (mTOR). The mTOR pathway acts as a central signalling hub, which is involved in a variety of cellular processes, such as cell metabolism and cell growth, as well as the differentiation, migration, and development of cells (Liu & Sabatini, 2020). mTOR is the central regulator and key modulator of myofibre growth and muscle mass as it both promotes protein synthesis (Ma & Blenis, 2009) and is suppressed by atrophy inducing signals (Yoon, 2017). mTOR has been shown to be involved in the growth of individual myofibres induced by external stimulation (Glass, 2005; Yoon, 2017). The absence of mTOR has been shown to lead to sever myopathy in mTOR knockout mice (Risson et al., 2009).

Several signalling pathways act as inputs to the mTOR signalling pathway, which thereby integrates both extracellular and intracellular signals. Among these signals are the presence and availability of nutrients, growth factors and hormones as well as the presence of oxygen and mechanical loading (Liu & Sabatini, 2020; You et al., 2019). Conversely, the disruption of the mTOR pathway can result in many diseases such as cancers, metabolic disorders, or autoimmune diseases (Kou et al., 2019; Perl, 2015), This can be for example in response to stress, changes in the presence of nutrients or hypoxia (Flück & Hoppeler, 2003; Sengupta et al., 2010).

The mTOR kinase acts as the catalytic subunit in two different complexes called mTOR complex 1 (mTORC1) and mTOR complex 2 (mTORC2). These vary not only in composition but also in their associated pathways, regulation, localisation, sensitivity to rapamycin and especially their function (Jhanwar-Uniyal et al., 2019). The complex

responsible for the regulation of myofibre size is mTORC1, which is also the better researched of the two complexes (Yoon, 2017).

1.3.1. mTOR complexes

The core components of the mTOR complex 1 (figure 2) are the mTOR kinase, the regulatory associated protein of mTOR (RAPTOR) and the mammalian lethal with Sec13 protein 8 (mLST8). RAPTOR plays a role in promoting the recruitment of substrates to mTORC1, by interacting with the substrates TOR signalling (TOS) motive (Hara et al., 2002; Kim et al., 2002; Kim et al., 2003). Several canonical targets of mTORC1 display this TOS motif and it is crucial for their regulation by mTOR (Schalm & Blenis, 2002). mLST8 - also known as GβL - interacts with mTOR and stabilizes the kinase activation loop (Kim et al., 2003). However, unlike RAPTOR it may not be essential for proper mTORC1 activity (Guertin et al., 2006). Further proteins are associated with mTORC1, such as proline-rich Akt substrate 40 kDa (PRAS40) and DEP domain containing mTOR interacting protein (DEPTOR). These act as inhibitory subunits, necessary for the regulation of mTOR activity. Furthermore, Rapamycin, a macrolide responsible for the naming of mTOR, acts as an inhibitor of mTORC1 activity. Rapamycin can interact with FK506-binding protein of 12 kDa (FKBP12), forming a complex which can bind do the FKBP12-Rapamycin binding domain (FRB) of mTOR (Huang et al., 2003; Huang & Houghton, 2001). This leads to an inhibition of mTOR and inhibits mTOR by preventing interaction with RAPTOR and its substrates (Cafferkey et al., 1993).

mTOR complex 2 (figure 2) is, similarly to mTORC1, comprising of mTOR, mLST8 and DEPTOR. mTORC2 does not have RAPTOR. Instead, rapamycin insensitive companion of mTOR (RICTOR) in combination with MAPK interacting protein 1 (mSIN1) and protein associated with RICTOR 1 and 2 (PROTOR 1/2) are responsible for the assembly of mTORC2. Furthermore, RICTOR blocks the FKBP12-rapamaycin complex, giving it its name as it makes mTORC2 insensitive to rapamycin. While the function of mTORC1 still remains less understood, it is involved in many processes such as cellular homeostasis, cell survival and cytoskeleton organization (Oh & Jacinto, 2011).

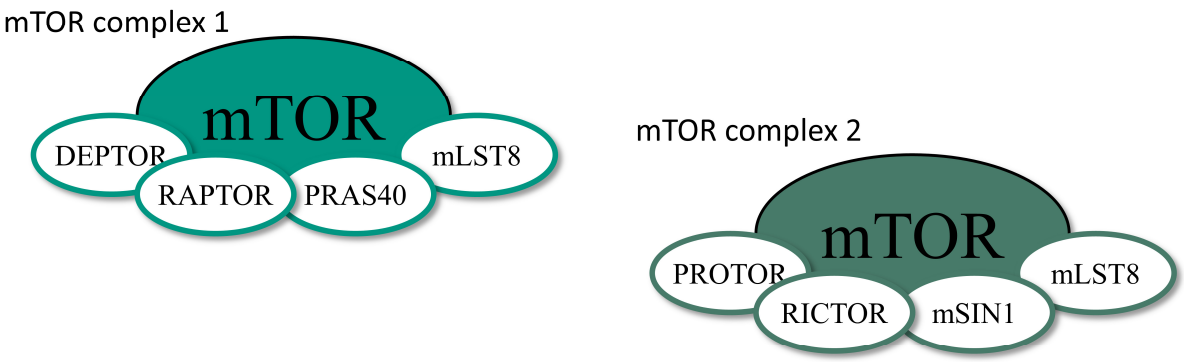

Figure 2: Schematic representation mTOR complex 1 and 2

mTOR complex 1 (mTORC1) comprised of mTOR, RAPTOR, mLST8, DEPTOR and PRAS40. mTOR complex 2 (mTORC2) comprised of mTOR, RICTOR, mLST8, DEPTOR, mSIN1 and PROTOR. Adapted from Norizadeh Abbariki, 2021.

1.3.2. mTORC1 function in muscle growth

mTORC1 plays an important role in muscle size. More specifically, mTORC1 activation has been shown to promote hypertrophy (Bodine et al., 2001; Marcotte et al., 2015). Indeed, IGF-1 and leucine induced myofibre hypertrophy depends on mTORC1 (Anthony et al., 2000; Rommel et al., 2001). Moreover, in mice, knocking out RAPTOR in skeletal muscle is associated with a severe muscle atrophy (Bentzinger et al., 2008). Furthermore, muscle activity itself, promoted by mechanical stimulation (Sancak et al., 2008; Sancak et al., 2010; Yoon, 2017) or by mechanical loading (Bodine et al., 2001; Sandri, 2008) has been shown to promote mTORC1 activation. Resistance exercise has been shown to induce hypertrophy in an mTORC1-dependent manner (Gonzalez, 2016; Terzis et al., 2008).

mTORC1 primarily promotes muscle growth through the regulation of protein synthesis (Bodine, 2022; You et al., 2019). mTOR stimulates protein synthesis on the one hand through translation initiation and on the other hand through ribosome biogenesis (Mayer & Grummt, 2006; Morita et al., 2015; Wang & Proud, 2006). mTORC1 has several downstream targets which it can phosphorylate upon activation. This is facilitated through RAPTOR, one of the components of mTORC1, which can interact with these substrates

through their TOS motif and helps facilitate their phosphorylation (Hara et al., 2002; Kim et al., 2002; Kim et al., 2003). Through the phosphorylation of its targets, mTORC1 can regulate metabolism, proliferation and ultimately cell growth by, on the one hand promoting the biosynthesis of proteins, lipids, nucleotides and ATP through various pathways and on the other hand inhibiting autophagy (Chauvin et al., 2013; Düvel et al., 2010; Gingras, Gygi, et al., 1999; Holz et al., 2005; Michels et al., 2010; Morita et al., 2013; Peterson et al., 2011; Porstmann et al., 2008; Rabanal-Ruiz et al., 2017).

Well known classical targets of mTORC1 activity are ribosomal S6 kinase B1 (S6K1) and eukaryotic initiation factor (eIF) 4E-binding proteins 1 (4E-BP1), important for translation initiation and protein synthesis (Gingras, Gygi, et al., 1999; Holz et al., 2005). However, other examples of downstream targets of mTORC1 are the sterol responsive element binding proteins (SREBP) (Porstmann et al., 2008) and lipin1 (Peterson et al., 2011), both of which are involved in lipid synthesis. Examples in other areas are the hypoxia-inducible transcription factor HIF-1α which is involved in glycolysis (Düvel et al., 2010) or MAF1 in ribosome biogenesis (Michels et al., 2010).

An important function of mTORC1 is promoting muscle growth, which it does through translation initiation by phosphorylating S6K1 and 4E-BP1. Activated mTORC1 interacts with and phosphorylates 4E-BP1. This phosphorylation leads to the inactivation of 4E-BP1 which releases its inhibitory interaction with the cap-binding eukaryotic initiation factor 4E (eIF4E). eIF4E promotes cap dependent translation by activating the eukaryote initiation factor 4F pre-initiation complex (eIF4F) (Gingras, Gygi, et al., 1999) (figure 3). eIF4F is necessary for cap-dependent translation, it is responsible for the recruitment of the small ribosomal subunit (40S) to the 5’ cap of mRNAs (Gingras, Raught, et al., 1999). mTORC1 further promotes translation initiation through the phosphorylation and activation of S6k1. While inactive S6K1 binds the eukaryotic initiation factor 3 complex (eIF3), phosphorylation of S6K1 releases eIF3 which acts as a scaffold for S6K1 and mTOR (Holz et al., 2005) as well as for eIF4F (Lefebvre et al., 2006). S6K1 can in turn phosphorylate various components associated with the translational machinery. Among these is programmed cell death protein 4 (Pdcd4). This phosphorylation leads to the

inactivation of Pdcd4 which releases translation initiation factors such as eIF4A, a part of the eIF4F complex (Dorrello et al., 2006)(figure 3).

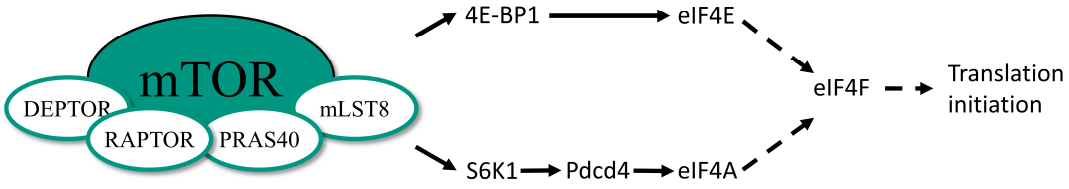

Figure 3: Schematic representation of translation initiation via mTORC1

mTORC1 phosphorylates its substrates 4E-BP1 and S6K1. 4E-BP1 releases its inhibition of eIF4E which can activate eIF4F. eIF4F is necessary for cap-dependent translation. S6K1 phosphorylates and inactivates Pdcd4. Pdcd4 releases eIF4A which acts as a scaffold for eIF4F.

mTORC1 can also promote muscle growth through the stimulation of ribosome biogenesis (von Walden et al., 2016; Wen et al., 2016). This allows for greater translational capacity and an increase in protein synthesis in myofibres. The increase in translation initiation through the phosphorylation of 4E-BP1 and S6K1 promotes ribosome biogenesis through the translation of ribosomal proteins and assembly factors (Chauvin et al., 2013; Holz et al., 2005).

Furthermore, mTORC1 can also promote the transcription of ribosomal RNA. There are four ribosomal RNAs the 5.8s, 18s and 28s (processed from 45s pre rRNA) and the 5s rRNA. These are transcribed by different RNA polymerases. The 45s pre rRNA is transcribed by the RNA polymerase I (Pol I), which is present in the nucleolus (Mayer & Grummt, 2006), while the RNA polymerase III (pol III) is responsible for the 5s rRNA and is located in the nucleus (Geiduschek & Tocchini-Valentini, 1988; Haeusler & Engelke, 2006). S6K1 can phosphorylate transcription intermediary factor 1 (TIF-1A) and upstream binding factor 1 (UBF), a rRNA transcription factor (Mayer et al., 2004; Panov et al., 2006). Both are key regulates of rRNA transcription via Pol I and through S6K1 are indirectly regulated by mTORC1 (figure 4). TIF-1A has been shown to play a key role in muscle hypertrophy, as extracellular stimulation through physical activity promotes rRNA

synthesis (Fyfe et al., 2018). mTORC1 has been further linked to rRNA transcription through its phosphorylation and inactivation of MAF1 (figure 4) a repressor of Pol III (Michels et al., 2010). It has been suggested that mTORC1 may promote myotube hypertrophy through a direct interaction with rDNA gene in the nucleolus (Tsang et al., 2010; von Walden et al., 2016).

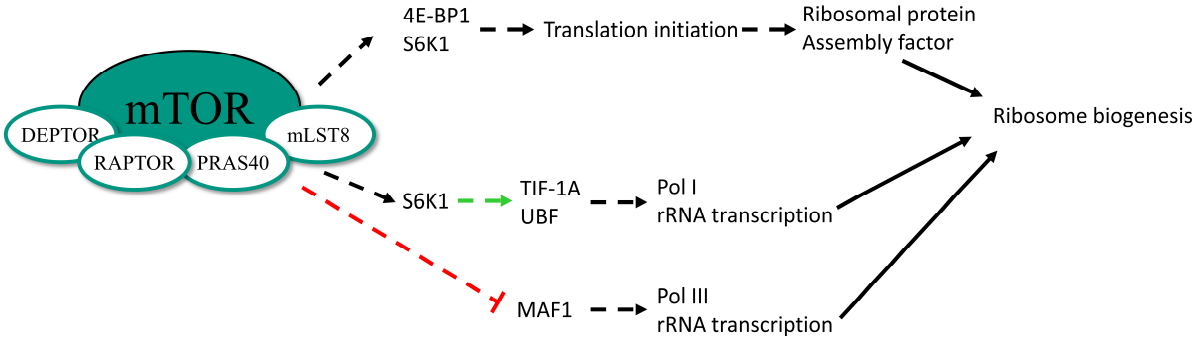

Figure 4: Schematic representation of mTORC1 regulating ribosome biogenesis.

mTORC1 phosphorylates its substrates 4E-BP1 and S6K1. This leads to translation initiation and promotes the translation of assembly factors and ribosomal proteins involved in ribosome biogenesis. S6K1 can activate TIF-1A and UBF which are regulators of Pol I rRNA transcription. mTORC1 can also phosphorylate and inhibit Maf1 directly lifting its repression of Pol III. This allows the transcription of the rRNAs necessary for ribosome biogenesis. These are possibilities of how mTORC1 can promote ribosome biogenesis.

1.3.3. mTORC1 activation

Various upstream signals including stress signals, the presence of nutrients, growth factors and amino acids can indirectly activate mTORC1 through several signalling pathways. The Insulin like growth factor I (IGF-I)/ Protein kinase B pathway is of importance for this activation (Huang & Manning, 2008; Rommel et al., 2001). Signalling through this pathway has been shown to be crucial in promoting muscle hypertrophy in an mTORC1-dependent manner (Glass, 2003).

The signalling cascades elicited through the various upstream signals converge to activate the small G-protein Ras homolog enriched in brain (RHEB). RHEB directly activates mTORC1 (Sato et al., 2009; Yang et al., 2006) (figure 5). RHEB is a part of the RAS family and localises at the surface of the lysosome (Angarola & Ferguson, 2019; Parmar & Tamanoi, 2010; Sancak et al., 2008). RHEB is a GTPase alternating between an active (GTP-bound) and inactive (GDP-bound) state. It is directly regulated by tuberous sclerosis complex 1 and 2 (TSC 1/ TSC 2 heterodimer). TSC1/2 binds to RHEB and keeps it in its GDP-bound, inactive, form. TSC2 is a GTPase-activating protein (GAP) and promotes hydrolysis of GTP to GDP (Huang & Manning, 2009). The signalling cascade leads to a phosphorylation of TSC1/2, facilitated by either Akt (Huang & Manning, 2009; Inoki et al., 2002) or ERK (Ma et al., 2005). This phosphorylation leads to the disassociation of TSC1/2 from RHEB. Following this disassociation RHEB can switch into the active GTP-bound state (figure 5). Active RHEB, along with other factors recruits mTORC1 to the membrane of the lysosome (Sancak et al., 2008; Sancak et al., 2010). At the lysosome RHEB activates mTORC1 by preventing the interaction between mTOR and an inhibitory binding protein (FKBP38) (Bai et al., 2007). It has also been suggested that RHEB may also interact directly with mTORC1 and activate it (Uhlenbrock et al., 2009). Subsequently, mTORC1 can recruit its substrates and phosphorylate them (figure 5).

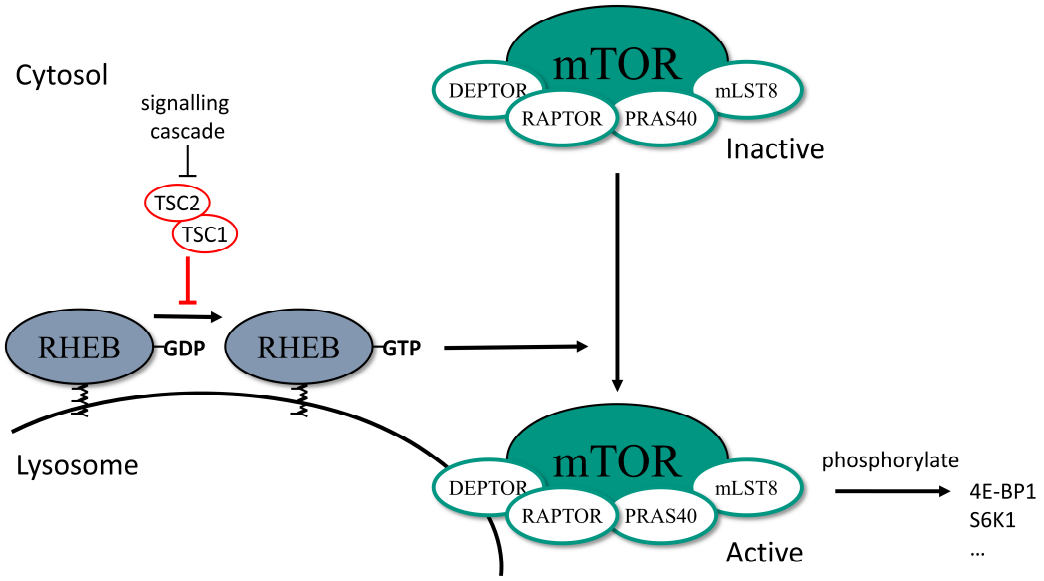

Figure 5: Schematic representation of mTORC1 activation

Signalling cascades lead to the phosphorylation and inactivation of TSC1/2. TSC1/2 dissociates from RHEB. RHEB can therefore switch to its active, GTP bound state and help recruit mTORC1 to the membrane of the lysosome. There RHEB can facilitate the activation of mTORC1 which can in turn phosphorylate its substrates.

1.4. RHEB

RHEB is ubiquitously expressed, however it derives its name from being initially identified in the brain of rats (Yamagata et al., 1994). RHEB is a small highly conserved (both in mammals and zebrafish) monomeric protein consisting of 184 amino acids and has a molecular weight of roughly 21 kDa. As the name further implies it is in the same family of small GTPases as RAS, RAP and RAL (Im et al., 2002). There are two RHEB genes RHEB1, and RHEB2 (also known as RHEB like 1 (RHEBL1)), which are expressed in different areas. RHEB1 is more ubiquitously expressed, nevertheless higher levels of expression have been seen in skeletal and cardiac muscles (Parmar & Tamanoi, 2010). The RHEB protein contains five G boxes, followed by a hypervariable region and a CAAX motif (figure 6). The five G boxes are conserved stretches of amino acids and are encoded in the first 169 amino acids from the N-terminus. Following this is a hypervariable region which acts as a short alpha helical linker comprised of 11 amino acids. The CAAX motif

follows the hypervariable region (figure 6) and is a signal for posttranslational modification (Parmar & Tamanoi, 2010).

The G boxes are GTP-binding and GTPase activity motifs and thus essential for correct binding and hydrolysis. The G1 box, which includes the phosphate-binding loop (P-loop), is the binding site for the guanine nucleotide. The G1 box interacts with the beta phosphate of GDP and GTP. The G2 box helps stabilizing this interaction by binding the terminal phosphate. The G2 box also partially coincides with the switch I region (figure 6). The G3 box further helps the guanine nucleotide binding by interacting with the nucleotide associated Mg^{2+} ion. The G3 box also partially coincides with the switch II region (figure 6). The G4 and G5 box play a role in the high-affinity binding of GTP and GDP. The G4 box is a major determinant of guanine nucleotide specificity. The G4 box interacts with the G1 box, thereby helping in stabilizing RHEB. The G5 box is also required for correct selection and binding by interacting with the guanine moiety (Osaka et al., 2021). RHEB possesses two switch regions (switch I and switch II), these are necessary for recognition by and interaction with GAPs or downstream effectors. Allowing RHEB to the change between its GTP- and GDP-bound form, thus acting as a molecular switch (Parmar & Tamanoi, 2010).

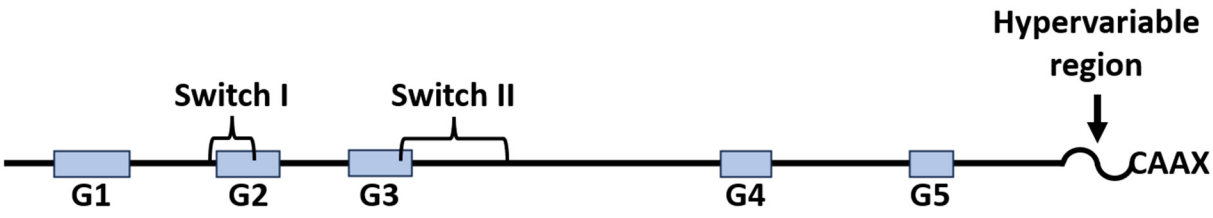

Figure 6: Schematic representation of RHEB

RHEB a 184 amino acid long protein consists of 5 G-boxes. Boxes 2 and 3 partially coincide with switch region I and II. At the end of RHEB there is a hypervariable region which acts as a linker followed by a CAAX motif. This motif is target of posttranslational farnesylation. Schematic adapted from an annotated amino acid sequence (Heard & Tamanoi, 2018).

While the switch I region can undergo conformational changes depending on the hydrolysis of GTP to GDP, the switch II region is only subjected to minor conformational changes (Parmar & Tamanoi, 2010). The switch I region contains an effector domain and is necessary for relaying its activity to downstream effectors (mTORC1). It allows the interaction between RHEB and the mTORC1 inhibitory protein FKBP38 and is necessary for mTORC1 activation. The switch II region is important due to its involvement in the GTP hydrolysis by the GAP activity of TSC2 (Mazhab-Jafari et al., 2012).

For the characterization of RHEB and its function, several RHEB mutants have been created. Several of these are located in the switch I or switch II region. A mutation in the switch region I, termed RHEB I39K, in which the isoleucine (I) is replaced with lysine (K), strongly reduces the interaction between RHEB and FKBP38. This allows for a functional RHEB, however strongly reduces the interaction with mTORC1 (Ma et al., 2008). A mutant termed RHEB Q64L, in which the glutamine (Q) in the switch II region has been replaced with a leucine (L), remains, due to this mutation, permanently bound to GTP and functions as a constitutively active RHEB (Li et al., 2004; Long et al., 2005). A further mutant with a mutation located in the switch II region is RHEB D60K in which the aspartic acid (D) is replaced with lysine (K), preventing the binding of GTP and GDP. This mutation results in a strong binding to FKBP38. Thus, FKBP38 stays bound to mTORC1 and RHEB D60K acts as a dominant negative mutant, competing with GTP-bound RHEB (Tabancay et al., 2003).

RHEB harbours a C-terminal CAAX motif, a cysteine (C) followed by two aliphatic amino acids (A) and a variable amino acid (X). This is a signal for a posttranslational modification, a farnesylation. The farnesyltransferase adds a farnesyl group to the CAAX motif. This farnesylation has been reported to promote localisation and attachment of RHEB to the membrane of the lysosome, endoplasmic reticulum or Golgi (Angarola & Ferguson, 2019; Buerger et al., 2006; Hanker et al., 2010; Sancak et al., 2008), which is in turn required for the activation of cytosolic mTORC1 (Buerger et al., 2006).

1.4.1. mTORC1-independent functions of RHEB

Besides its role in activating mTORC1 in the cytosol, RHEB has also been shown to exert several mTORC1-independent functions (Karbowniczek et al., 2006; Karbowniczek et al., 2010; Lacher et al., 2010; Meng et al., 2019; Sato et al., 2015). Notably, RHEB is involved in the Notch pathway. In brown and beige adipose tissue RHEB has been reported to selectively activate Notch signalling and to promote protein kinase A (PKA) signalling (Meng et al., 2019). Thus, RHEB controls the expression of thermogenic genes through an mTORC1-independent mechanism. RHEB is further involved in the Notch signalling pathway, regulating Notch signalling in Drosophila sensory organ precursor (SOP) cells. Inactivation of TSC1 or overexpression of RHEB led to a switch in SOP cell fate decision, indicating the activation of Notch and Notch target genes by RHEB. Furthermore, the experiments indicated that this activation was in an mTORC1 independent manner, as the use of rapamycin or downregulation of RAPTOR showed no effect on the Notch activation (Karbowniczek et al., 2010). In the RAS-RAF-MEK signalling pathway RHEB has been shown to inhibit the B-RAF kinase. This impacts its ability to associate with RAS and C-RAF and prevents B-RAF and C-RAF heterodimerization (Karbowniczek et al., 2006). RHEB has also been shown to have several mTORC1-independent downstream effectors such as carbamoyl-phosphate synthetase 2, aspartate transcarbamoylase, and dihydroorotase (CAD) (Sato et al., 2015). Interestingly, 5' adenosine-monophosphate-activated protein kinase (AMPK), an enzyme which inhibits protein synthesis and promotes muscle atrophy (Afinanisa et al., 2021) is also an mTORC-1-independent effector of RHEB (Lacher et al., 2010). Whether these mTORC1-independent functions of RHEB are conserved in zebrafish and whether they are involved in the control of muscle growth is unknown.

1.4.2. Nuclear functions of RHEB

Besides its canonical role in the activation of mTORC1 in the cytosol, RHEB might also exert nuclear functions. RHEB, mTOR and some mTORC1 components have indeed been observed in the nucleus of cells in culture (Zhong et al., 2022). Furthermore, RHEB

and mTOR have been shown to interact in the nucleus (Yadav et al., 2013), and a growth factor-stimulated mTORC1 activity, as measured by a FRET sensor has been detected in the nucleus of cultured fibroblasts (Zhou et al., 2015). Interestingly, this activity was stimulated by treatment with a growth factor (Zhong et al., 2022). However, the physiological role of such a nuclear RHEB-induced mTORC1 activity is unknown. In particular, whether this nuclear activation of mTORC1 also occurs in skeletal muscle and whether it plays a role in muscle growth is unknown.

Previous results from the laboratory (Norizadeh Abbariki, 2021) showed that RHEB not only has a nuclear function in muscle growth in zebrafish, RHEB also has a mTORC1-independent function. The results indicate that in zebrafish embryo, nuclear RHEB promotes muscle growth. Over-expression, selectively in myofibres, of the constitutively active mutant RHEB Q64L targeted to the nucleus by the use of a nuclear localisation signal (NLS) resulted in an increase in myofibre volume. This increase occurred without any modification of the number of myonuclei, indicating that nuclear RHEB promotes hypertrophy and not hyperplasia. Conversely, the dominant negative mutant RHEB D60K harbouring an NLS resulted in a reduction in myofibre volume. The use of rapamycin to inhibit mTORC1 and of the RHEB I39K mutation showed that the hypertrophy promoting effect of nuclear RHEB is mTORC1-independent (Norizadeh Abbariki, 2021).

Furthermore, while RHEB was mostly detected in the cytosol of adult zebrafish myofibres, it was strongly enriched in the nucleus of embryonic myofibres (Norizadeh Abbariki, 2021). This result suggests a regulation of RHEB subcellular localisation during zebrafish development. Interestingly, while RHEB farnesylation is required for its anchoring to endomenbranes and the activation of mTORC1 in the cytosol (Angarola & Ferguson, 2019), inactivating farnesyltransferase through the use of an inhibitor (Hanker et al., 2010) or mutation of the CAAX motif (Takahashi et al., 2005) results in RHEB localising in the nucleus. Furthermore, farnesylation of RHEB is not necessary for the activation of nuclear mTORC1 (Zhong et al., 2022). Thus, one might hypothesize that the regulation of RHEB farnesylation plays a role in the regulation of its subcellular localisation and therefore in its nuclear functions.

1.5. Hypotheses and aims

Previous results of the laboratory (Norizadeh Abbariki, 2021) showed that in adult zebrafish myofibres RHEB is primarily located in the cytosol, whereas it is strongly expressed in the nucleus of myofibres in the early embryo. This observation suggests a regulation of RHEB subcellular localisation during muscle development and/or myofibre maturation. My first aim was to investigate the precise timing of the change in RHEB subcellular localisation as a first step towards elucidating the underlying mechanism. Furthermore, at early embryonic stages, zebrafish skeletal muscle is composed of immature myofibres with very little contraction. Then skeletal muscle activity strongly increases when myofibres mature and contract more frequently. This, together with my first results prompted me to investigate the effect of skeletal muscle activity on RHEB subcellular localisation. Finally, given the critical role of farnesylation in determining RHEB subcellular localisation, I investigated whether it is involved in the change of RHEB localisation in myofibres.

2. Materials and Methods

2.1. Materials

2.1.1. Consumables

Consumables	Company
6 well plate	Greiner
35 mm glass bottom plate	Greiner
12 mm glass coverslip	Epredia

All cell culture consumables, unless otherwise stated, were obtained from Greiner Bio-One GmbH, Frickenhausen, Germany.

2.1.2. Chemicals

Chemicals	Company
Lonafarnib	Sigma (Merck)
Phenol red	Sigma (Merck)
PTU (N-Phenylthiourea)	Sigma (Merck)
Tricaine (Ethyl 3-aminobenzoate methanesulfonate salt)	Sigma (Merck)
BSA (HyClone Bovine Serum Albumin)	Cytiva
DAPI (4′,6-Diamidin-2-phenylindol)	Sigma (Merck)

All other chemicals, unless otherwise stated, were obtained from Carl Roth GmbH + Co. KG, Karlsruhe, Germany; Thermo Fisher Scientific GmbH, Dreieich, Germany or Merck KGaA, Darmstadt, Germany.

2.1.3. Kits

Kit	Company
mMESSAGE mMACHINE (SP6 Transkriptionskit)	Invitrogen
Plasmid Midi Kit	Qiagen

2.1.4. Hardware

Device	Company
Micropipette puller	Sutter Instruments
Micro injector MINJ-D	Tritech Research
C-Dish 6 well	Ion Optix
C-Pace EM	Ion Optix
LSM 900	Zeiss

2.1.5. Antibodies

2.1.5.1. Primary

Name	Isotype	Dilution	Company (Ordernumber)
Anti-RHEB (E1G1R)	Rabbit	1:50	Cell Signaling (#13879)
Anti-Fibrillarin (38F3)	Mouse	1:200	Novus Biology (NB300-269)
Anti-Fibrillarin (38F3)	Mouse	1:200	Merck (MABE1154)

2.1.5.2. Secondary

Name	Isotype	Dilution	Company (Ordernumber)
Alexa Fluor 546 – conjugated anti-rabbit	Goat	1:1000	Thermo Fischer (A-11010)
Alexa Fluor 488 – conjugated anti-mouse	Goat	1:1000	Thermo Fischer (A-11001)

2.1.6. Buffers

2.1.6.1. Immunofluorescent staining

Buffer	Contents
Fixation buffer	4 % Formaldehyde in PBS -/-
Blocking buffer	5 % BSA, 1 % DMSO, 0,1% Tween 20 in PBS -/-
Wash buffer	0,1% Tween 20 in PBS -/-

2.1.7. Zebrafish and medaka strains and medium

2.1.7.1. Zebrafish strains

The zebrafish wildtype (ABO) and mutant embryos were obtained from the KIT fish facility (B319).

Mutation name	Genotype	ZFIN Genotype
Steif	unc45b het incross	unc45b $^{sb60/sb60}$ (AB)
fixe	AB_ZIRC_KA2 X fixe	chrnd $^{sb13/+}$ (AB, ABO)

2.1.7.2. Medaka strain

The medaka wildtype (iCab) embryo was obtained from the group of Felix Loosli (KIT IBCS-BIP)

2.1.7.3. Fish Media

Media	**Recipe**
E3 media (60x)	17.2 g NaCl, 0.76 g KCL, 2.9 g $CaCl_2x2H_2O$ and 4.9 g $MgSO_4x7H_2O$ in 1 l dd H_2O
ERM media (100x)	100 g NaCl, 3 g KCL, 4 g $CaCl_2x2H_2O$ and 16 g $MgSO_4x7H_2O$ in 1 l dd H_2O
PTU (N-Phenylthiourea) (100x)	0.3 % dissolved in dd H_2O
Tricaine 20x	400 mg Tricaine, 2.08 ml Tris Base, 100 ml dd H_2O, pH adjusted to 7.0

2.1.8. Bacterial strain and media

2.1.8.1. Bacterial strain

DH5α – a strain of chemically competent *E. coli*

2.1.8.2. Bacterial media

Media	Recipe
LB (Lysogeny Broth)	10 g Tryptone, 5 g Yeast extract, 10 g NaCl in 1 l of dd H_2O (pH set to 7.5)
LB Agar (Lysogeny Broth + Agar)	4 g Tryptone, 2 g Yeast extract, 4 g NaCl, 8 g Agar-Agar, in 400 ml of dd H_2O
S.O.C (SOB (Super Optimal Broth) + glucose)	20 g Tryptone, 5 g Yeast extract in 1 l dd H_2O + 10 mM NaCl, 2,5 mM KCl, 10 mM $MgCl_2$, 10 mM $MgSO_4$, 20 mM Glucose

2.1.9. Genetic tools

2.1.9.1. Plasmids

Plasmid	Function
PC2 alpha-Bungarotoxin	Vector containing α-Bungarotoxin sequence for mRNA generation and subsequent injection. α-Bungarotoxin binds to nicotinic acetylcholine receptor preventing binding of acetylcholine

2.1.9.2. Morpholino

Name	Function	Sequence	Company
smoc2 (ATG) Mo cont	Morpholino control	ctggctcacttagtggatcgaccat	GeneTools
ZfRheb Mo	Morpholino against zebrafish RHEB	ctgcggcatctttatttactcccta	GeneTools

2.2. Methods

2.2.1. DNA and RNA

Plasmid DNA for the creation of mRNA was transformed in competent cells and a plasmid preparation was performed. Subsequently the plasmid was used for mRNA transcription.

2.2.1.1. Transformation

50 µl of the chemically competent *E. coli* strain DH5α were thawed (on ice). Following this 1 µl of the plasmid DNA was added and incubated for 30 minutes on ice. This was followed by a 45 second heat shock at 42°C with subsequent cooling for 2 minutes on ice. After this 500 µl of S.O.C-Medium was added to the mix and it was incubated for 1 hour at 37°C. Following the incubation 100 µl of the mix was plated on LB agar plates containing the necessary 50 µg/ml Ampicillin for selection. After 24 hours incubation at 37°C a single colony was picked and placed into 100 ml of LB media containing 50 µg/ml ampicillin and incubated for a further 24 hours at 37°C. A plasmid preparation was performed with the pellet from these cells.

2.2.1.2. Plasmid preparation

The plasmid preparation was performed using the Midi prep kit from Qiagen and following the manufacturer's instructions. After final centrifugation the pellet was resuspend in TE buffer. Following the preparation, the concentration of the DNA was adjusted to 1 µg / µl and frozen at -20°C for storage.

2.2.1.3. mRNA transcription

mRNA transcription was performed on linearized PC2 alpha-Bungarotoxin plasmid using the mMessage mMachine SP6 kit. After transcription the mRNA content was measured and frozen at -80°C until used in micro-injection.

2.2.2. Fish methods

2.2.2.1. Ethics statement

The animal husbandry for zebrafish (Danio rerio) and medaka (Oryzias latipes) was carried out in compliance with the German Animal Welfare Act. It was approved by the Regierungspräsidium Karlsruhe, Germany under the permits Aktenzeichen 35-9185.64/BH KIT and 35-9185.64/BH IBCS-BIP. For the experimental procedures or euthanasia no permits were required, as any such procedures were performed before animals were capable of independent feeding (5 days post fertilization for zebrafish and 10 days post fertilization for medaka).

2.2.2.2. Zebrafish husbandry

Adult zebrafish were kept in a one-to-one ratio of female to male fish in tanks with a recirculating water system kept at 28.5 °C. A constant light-dark cycle of 14 h light 10 h dark was maintained. Feeding was done twice daily with commercial dry food and additionally once a day with brine shrimp (live food) hatched in-house.

2.2.2.3. Medaka husbandry

Adult medaka were kept in a one-to-one ratio of female to male fish in tanks with a recirculating water system kept at 26 °C. A constant light-dark cycle of 14 h light 10 h dark was maintained. Feeding was done twice daily with commercial dry food and additionally once a day with brine shrimp (live food) hatched in-house.

2.2.2.4. Zebrafish breeding

Zebrafish breeding was performed in the KIT zebrafish fish facility in building 319. The afternoon before breeding male and female zebrafish were separated pairwise into small tanks. Male and female separated by a clear divider. The following morning the divider

was removed, allowing zebrafish mating (this was only done once the light cycle had begun). After ~ 20 minutes the zebrafish eggs were collected. The collected eggs were sorted and fertilized eggs were kept in 100 mm petri dishes filled with 1x E3 buffer in an incubator of 28°C with 14 hours light 10 hours dark cycle.

2.2.2.5. Medaka breeding

Medaka eggs were obtained from the group of Felix Loosli (KIT IBCS-BIP). Breeding was performed in the KIT medaka fish facility. Eggs were kept in 100 mm petri dishes with 1x ERM buffer in an incubator of 28°C with 14 hours light 10 hours dark cycle.

2.2.2.6. Zebrafish micro-injection

The needles for injection were made using a micropipette puller and glass capillary tubes with a filament (borosilicate glass, 0,58 mm). In preparation of injection the mRNA or morpholino was prepared via dilution in dd H_2O and supplemented with phenol red as a visibility marker.

Injected material	**Final concentration / molarity**	**Phenol red**
α-Bungarotoxin mRNA	100 ng/µl	0,1%
Morpholino (smoc cont & zfRHEB)	0,4 mM (1:5 dilution)	0,1%

Micro-injection was performed on fertilized eggs in the single cell stage. The eggs were injected (using the micro injector MINJ-D) through the chorion into the single cell, with a drop of the prepared injectant (mRNA or morpholino) approximately 10 % the size of the cell. After injection the eggs were incubated and raised at 28°C 14 h light 10 h dark in a petri-dish with 1x E3 buffer.

2.2.2.7. Zebrafish selection

2.2.2.7.1. *steif* mutant selection

Heterozygous zebrafish carrying one copy of the unc45b mutation (+/-), were used for crossing (no effect on phenotype). The expected outcome of this crossing was homozygous (-/-) *steif* mutant embryos carrying two copies of the mutation and resulting in paralysis and a change in phenotype, heterozygous (+/-) embryos carrying one copy of the mutation, and homozygous (+/+) wildtype embryos.

For selection of the homozygous (-/-) *steif* mutant embryos, several factors were observed. Changes in phenotype (disorganization of the myofibers), as well as a lack of early random twitching and overall movement, as well as a lack of a heartbeat and a lack of a touch response. These *steif* mutant embryos were pre-sorted at 1 dpf and checked at 2 and 3 dpf. Due to the lack of movement in the *steif* mutants the embryos had to be manually dechorionated. This was done at 2 dpf to allow embryos to slowly straighten, as a lack of motility results in embryos being curved due to the chorion directly after dechorionation.

The heterozygous (+/-) embryos, as well as the homozygous (+/+) wildtype embryos, showed no change in phenotype or behaviour. From these the control embryos were carefully chosen.

2.2.2.7.2. *fixe* mutant selection

Heterozygous zebrafish carrying one copy of the chrnd mutation (+/-), were used for crossing. The expected outcome of this crossing was: homozygous (-/-) *fixe* mutant embryos carrying two copies of the mutation resulting in immobilization, heterozygous (+/-) embryos carrying one copy of the mutation, and homozygous (+/+) wildtype embryos.

For selection of the homozygous (-/-) *fixe* mutant embryos, several factors were observed. They were selected by observation of a lack of early random twitching and overall

movement, as well as a lack of a touch response. These *fixe* mutant embryos were pre-sorted at 1 dpf and checked at 2 and 3 dpf. Due to the lack of movement in the *fixe* mutants the embryos had to be manually dechorionated. This was done at 2 dpf to allow embryos to slowly straighten, as a lack of motility results in embryos being curved due to the chorion directly after dechorionation.

The heterozygous (+/-) embryos, as well as the homozygous (+/+) wildtype embryos, showed no change in phenotype or behaviour. From these the control embryos were carefully chosen.

2.2.2.7.3. α-Bungarotoxin immobilization selection

Zebrafish embryos injected with α-Bungarotoxin were sorted, injected embryos were expected to show similar behaviour to the *fixe* mutants. Only embryo showing no random twitching or movement and no touch response after sorting at 1 dpf, 2 dpf and 3 dpf were chosen as “α-Bungarotoxin injected” embryos. Due to the lack of movement the embryos had to be manually dechorionated at 2 dpf to allow embryos to slowly straighten, as a lack of motility results in embryos being curved due to the chorion directly after dechorionation.

2.2.2.8. Zebrafish treatment

2.2.2.8.1. PTU treatment

To increase transparency of zebrafish embryos they were dechorionated and subsequently treated with PTU (1-phenyl 2-thiourea) preventing pigmentation and thus increasing transparency. 100x PTU buffer was diluted to a final 1x concentration in E3 buffer (0,003% PTU in 1x E3). Zebrafish embryos were kept in this buffer in a 100 mm petri dish after 1 dpf.

2.2.2.8.2. Tricaine treatment

To prevent zebrafish muscle activity zebrafish embryos were dechorionated and subsequently treated for multiple days in tricaine. Tricaine (4 g per l) was diluted 1:40 in E3 buffer (for short-term anesthetizing a dilution of 1:20 is used). At 1 dpf zebrafish embryos were placed in this long-term anesthetizing buffer and incubated. Proper anesthetisation was tested daily (lack of random movement and touch response). Long term anesthetizing buffer was replenished daily.

2.2.2.8.3. Lonafarnib treatment

To prevent farnesylation zebrafish embryos were dechorionated and subsequently treated with the farnesyl transferase inhibitor (FTI) lonafarnib. Embryos were placed into small wells (24 well plate) at 24 hpf and treated with 40 µM lonafarnib in 1xE3 (dilution 1:250 from 10 mM stock). Lonafarnib was replaced each day.

2.2.2.8.4. Electrical pulse stimulation

Electrical pulse stimulation (EPS), adapted from Kilroy et al., 2022 was performed on zebrafish embryos starting at 17 hpf. In preparation 6 well chambers well filled ¾ with 1% agarose in E3 medium. After cooling, agarose was cut to make space for the electrodes of the 6-well C-Dish electrode element (Ion Optix) (figure 7). Furthermore, small wells were cut into the agarose, perpendicular to the electrodes (figure 7). After filling the wells with E3+Hepes (0,01%) the 17 hpf old embryos were dechorionated and carefully placed into the small wells. The plate was carefully placed in an incubator and the C-Dish connected to the C-Pace power supply. Movement was induced through pulsing for 1 second (10 x 10 ms pulse + 90 ms wait at 7 V), this was followed by an 8-hour resting period. After roughly 20 hours the media was replaced and a new C-Dish electrode element was used, as overuse of both can affect media quality. At 48 hpf, the embryos were removed and used for further experiments, e.g. wholemount fixation.

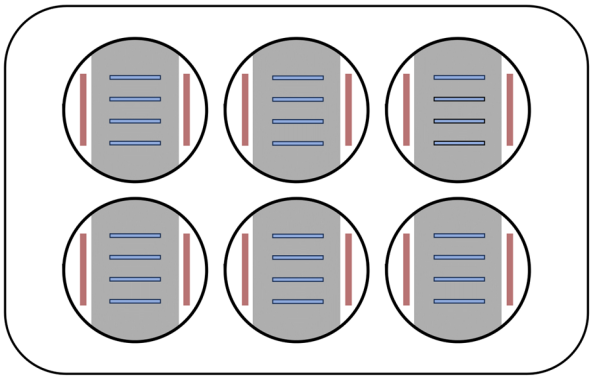

Figure 7: Setup for electrical pulse stimulation in 6-well plates

6-well plate for electrical pulse stimulation. Filled with agarose (in grey) ¾ of the height of the well. Space cleared from agarose for the electrodes (in red) and small wells (in blue) made perpendicular to the electrodes in which the embryos are placed.

2.2.3. Wholemount fixation and immunofluorescence

2.2.3.1. Wholemount fixation

2.2.3.1.1. Zebrafish wholemount fixation

1 and 2 dpf old zebrafish embryos were dechorionated prior to fixation (if not already dechorionated for treatment). For fixation the zebrafish embryos (1, 2 and 3 dpf) were euthanized through anesthetization via tricaine. After euthanasia the embryos were placed in 4% formaldehyde (diluted in PBS -/-) for 30 minutes (longer fixation prevented proper immunoreactivity of the anti-RHEB E1G1R antibody). After fixation the embryos were washed for 5 minutes in PBS -/- before immunofluorescent staining.

2.2.3.1.2. Medaka wholemount fixation

Hatched medaka (7 and 8 dpf) were fixed using the same method as for zebrafish embryos. Unhatched medaka embryos were fixed in the chorion in 2% formaldehyde (in PBS -/-) over night at 4°C. After fixation the embryos were placed in PBS -/- and dechorionated. After an additional 5-minute wash in PBS -/- immunofluorescent staining was performed.

2.2.3.2. Immunofluorescent staining

After fixation and subsequent washing immunofluorescent staining was performed. For this the embryos were permeabilized by incubating at -20°C in cold acetone (stored at -20°C). The incubation time depended on the age of the embryos:

Species	Age	Incubation duration
Zebrafish	1 dpf	7 minutes
Zebrafish	2 dpf	8 minutes
Zebrafish	3 dpf	9 minutes
Medaka	4, 5, 6, 7 and 8 dpf	9 minutes

After permeabilization embryos were washed 5 times for 5 minutes in PBS -/-. Following this they were blocked for 4 hours at room temperature in blocking buffer. After blocking the embryos were incubated over night at 4°C with the primary antibody diluted in blocking buffer. The following day the embryos were washed 5 times for 10 minutes at room temperature with wash buffer. After washing the embryos were incubated over night at 4°C with the secondary antibody diluted in blocking buffer. The following day the embryos were washed 3 times for 10 minutes in wash buffer, following this they were washed again 3 times for 5 minutes in PBS -/-. Finally, the embryos were incubated in DAPI (1 µg / ml in PBS -/-). After incubating a minimum of 30 minutes at room temperature microscopy could be performed on the embryos. Otherwise, they were stored at 4°C for later microscopy.

2.2.4. Microscopy, image analysis and statistical analysis

2.2.4.1. Microscopy

Performed on zebrafish and medaka embryos after wholemount immunofluorescent staining (see 2.2.3). For microscopy of the embryos, they were placed in a 35 mm glass bottom plate with a few drops of PBS -/-, after which a 12 mm glass coverslip was carefully

placed on top (to ensure contact with the bottom glass plate and better microscopy). Confocal microscopy was performed using either a 40x oil immersion objective or a 63x oil immersion objective on a Zeiss LSM 900. Microscopy images were taken with lasers (405 nm, 488 nm and 561 nm) and filters appropriate for the secondary antibodies and dyes (Alexa 488, Alexa 546 and DAPI). In the microscope the muscles of the zebrafish embryos were observed, however for consistency and due to possible deviations in development the images were only taken from the first third of the muscle area (figure 8).

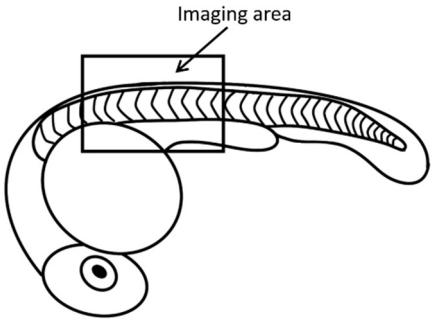

Figure 8: Microscope imaging area

Images of myofibres were only taken in the shown imaging area. This was done to keep consistency and to prevent possible effects of different development in different areas.

2.2.4.2. Image analysis

For image analysis and subsequent statistical analysis, the surface area and signal intensity of the myofibre and nucleus was measured. Image analysis was done using the Fiji ImageJ software package version 2.14.0/1.54f (Schindelin et al., 2012). Of importance for this was the choice of the myofibres. Each image shows a multitude of myofibres, however, only myofibres that were in the focal plane were used. Furthermore, only myofibres that had a clear in-focus nucleus (as seen with the DAPI channel) were used. Single myofibres were selected manually and the surface area and signal intensity of RHEB channel was acquired. For the nuclear signal, the selection of the nuclear area was manually performed in the DAPI channel (or a composite). The measurement of the values for area size and signal intensity was performed in the RHEB channel.

The surface area and signal intensity of the cytosol was obtained mathematically, by subtracting area and signal intensity of the nucleus from that of the whole myofibre. After this the average signal intensity of the cytosol and the nucleus was calculated by dividing

the signal intensity by the area. The average signal intensities were then used to create a ratio of average nuclear signal intensity to average cytosolic signal intensity. Where possible the experiment represented at least 30 myofibres from 7 fish embryos from 3 experiments. This ratio was displayed in a boxplot.

2.2.4.3. Statistical analysis

The statistical significance was determined by using a two-sided students t-test. A p-value of $P < 0.05$ considered sufficient to reject the null hypothesis. In experiments in which multiple comparisons were performed a Bonferroni correction was applied.

3. Results

3.1. Subcellular localisation of RHEB in zebrafish muscle

Given the previous results from the laboratory showing that in the myofibre of two-day old zebrafish embryo RHEB localises to the nucleus while it is exclusively cytosolic in adult myofibres (Norizadeh Abbariki, 2021), I first investigated the timing of this change in subcellular localisation of RHEB during muscle development in zebrafish embryo.

3.1.1. Localisation of RHEB in muscle during zebrafish development

As RHEB was reported in the nucleus of zebrafish myofibres at 2 days post fertilization (2 dpf) I first investigated the localisation of RHEB during the first days of zebrafish development. For this a wholemount immunofluorescent staining was performed at 1, 2 and 3 dpf. During the first two days of zebrafish development RHEB was indeed present in the nuclei of the myofibres (figure 9a). At 3 dpf there was a reduction in this nuclear presence of RHEB (figure 9a). Notably, starting at 2 dpf the cytosolic signal of RHEB seemed stronger and RHEB started to accumulate around the z-band of the sarcomere. In the nucleus, RHEB was strongly enriched in the nucleolus at 1 and 2 dpf, as shown by its co-localisation with fibrillarin used as a nucleolar marker. In several images this nucleolar enrichment persisted at 3 dpf, a time point when RHEB nuclear localisation had strongly decreased. These results show that RHEB is in the nucleus during early zebrafish development, a shift occurring between two- and three-days post fertilization in which the nuclear RHEB decreases. To confirm these results a quantification of the signal was performed (figure 9b). This quantification compares the overall intensity of the nuclear RHEB signal with the cytosolic RHEB signal of single myofibres (shown as a ratio). Indeed, the quantification shows that at 1 and 2 dpf there is a strong nuclear RHEB signal with no significant change between these two days. At 3 dpf there was a significant reduction of the ratio. Zebrafish hatch between 2 dpf and 3 dpf, changing from embryo to larvae. Thus, these results show the presence of nuclear RHEB in the myofibres of embryonic zebrafish (1 and 2 dpf) and is reduced in zebrafish larvae.

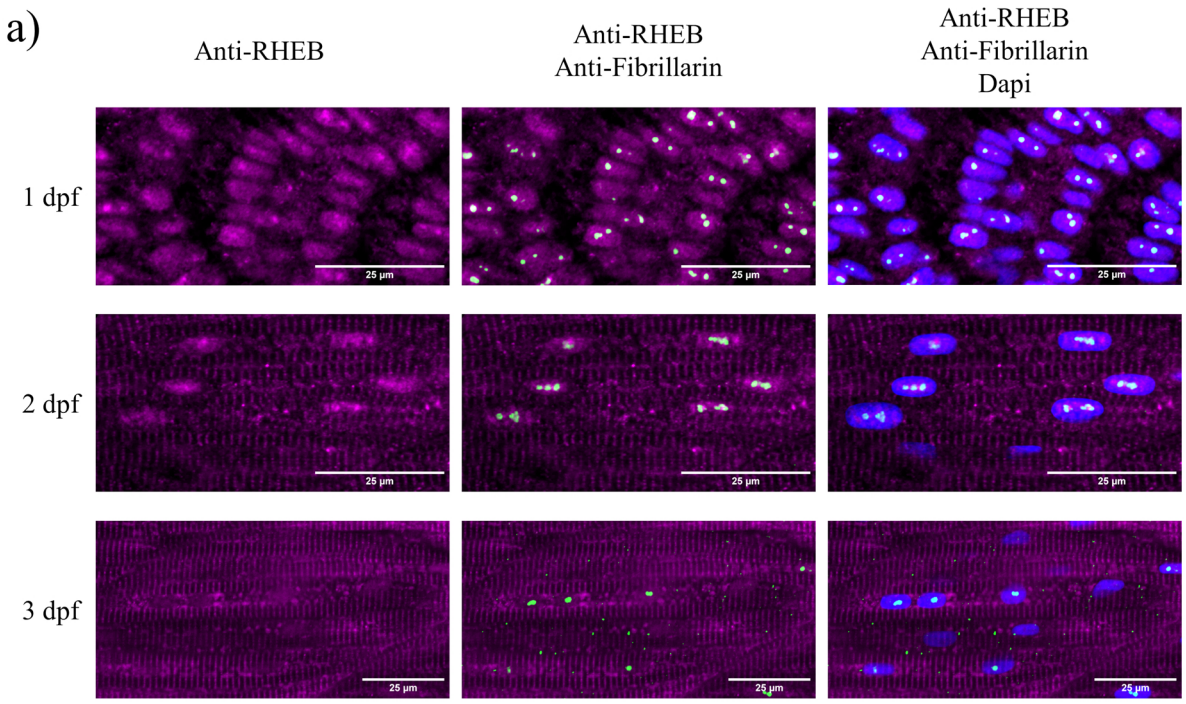

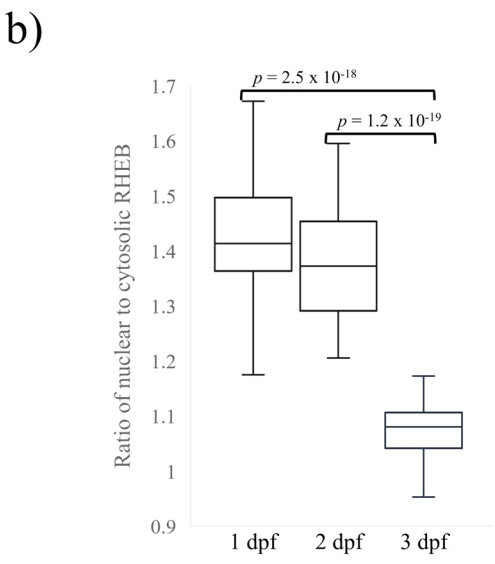

Figure 9: Subcellular localisation of RHEB during zebrafish muscle development

Zebrafish embryo at 1 dpf, 2 dpf and larvae at 3 dpf were subjected to a wholemount immunofluorescent analysis using an antibody against RHEB (magenta) and Fibrillarin (green). DAPI was used for counterstaining of the nuclei (blue). **a**) Representative confocal microscopy images are shown (scale bar: 25 µm). **b**) The ratio of the mean signal intensity of RHEB in nuclei (nuclear signal normalized to nucleic surface area) to the mean signal intensity in the cytosol (cytosolic signal normalized to cytosolic surface area) is presented as a box and whiskers plot. For each group at least 30 single myofibres from at least 7 animals were analyzed. Bonferroni adjusted α: *p<0.01667.*

The co-localisation of the anti-RHEB antibody and the anti-fibrillarin antibody in the nucleolus shows that indeed the antibodies can penetrate the different cell layers and subcellular structures. However, to validate the antibody (anti-RHEB E1G1R) and test its specificity, a RHEB knockdown experiment was performed using a morpholino oligonucleotide. For the experiments single cell stage zebrafish embryos were injected with either a RHEB or control morpholino. At 3 dpf a wholemount immunofluorescent staining against RHEB was performed. Indeed, while RHEB was clearly visible in zebrafish embryos injected with the control morpholino (figure 10), there was an almost complete reduction of the signal in the zebrafish embryos injected with the RHEB morpholino (figure 10). Thus, the RHEB antibody is indeed specific in zebrafish. However, a strong RHEB immunoreactivity was still visible in myofibre nucleoli in the zebrafish injected with the RHEB morpholino.

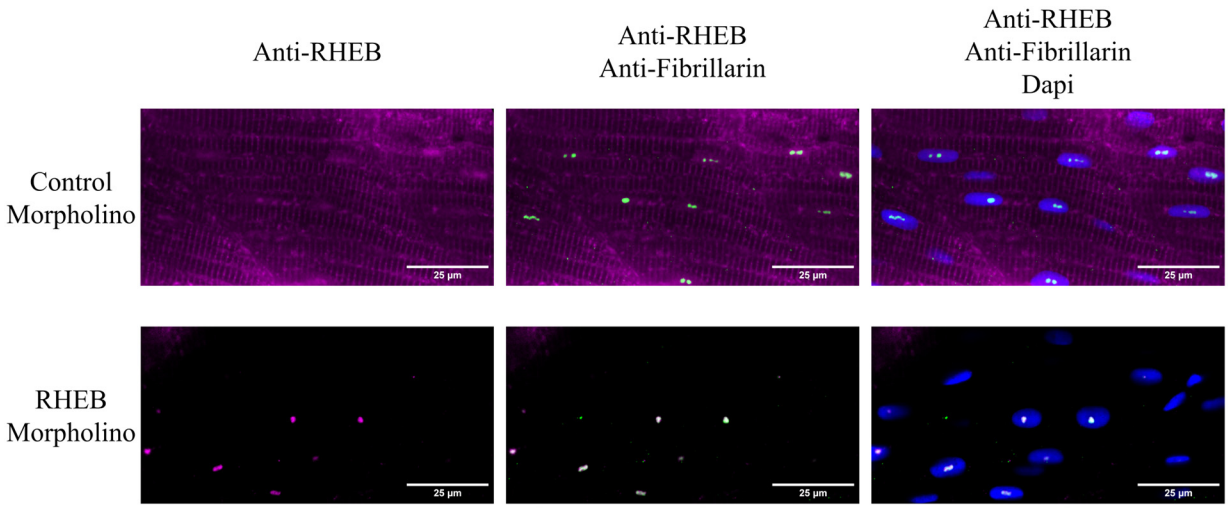

Figure 10: Effect of RHEB morpholino on RHEB antibody binding in zebrafish embryo

Single cell stage zebrafish embryos were injected with either a control morpholino or a RHEB morpholino. At 3 dpf the zebrafish larvae were subjected to a wholemount immunofluorescent analysis using antibodies against RHEB (magenta) and Fibrillarin (green). DAPI was used for counterstaining of the nuclei (blue). Representative (6 animals of each condition) confocal microscopy images of muscles are shown (scale bar: 25 µm).

3.1.2. Localisation of RHEB in muscle during medaka development

As the localisation of RHEB in zebrafish changed around the timepoint of hatching, the question arose whether this change could indeed be connected to hatching. Therefore, I studied the subcellular localisation of RHEB in a different model organism. *Oryzias latipes,* also known as medaka (or Japanese rice fish), was chosen for these experiments. Both medaka and zebrafish belong to the teleost group. Medaka are similar in size to zebrafish and offer similar advantages as a model organism, the embryo being nearly transparent, easy to observe and handle.

However, medaka development is slower, segmentation starting at 27 hpf (Iwamatsu, 2004), whereas in zebrafish it starts at 10 hpf (Kimmel et al., 1995). Furthermore, hatching in medaka occurs at a later timepoint, between 6 and 7 dpf under our husbandry conditions. In medaka embryos, RHEB was detected in the nucleus of myofibres until 6 dpf (figure 11a). After hatching, at 7 dpf and 8 dpf, there was a reduction in nuclear RHEB. These results indeed mirror those in zebrafish, a change in localisation occurring between embryonic and larval stage. As with zebrafish, there was a localisation of RHEB around the z-band of the sarcomere at later stages (7 and 8 dpf). As opposed to zebrafish, no nucleolar RHEB immunoreactivity was observed in medaka myofibres. As with the zebrafish a quantification was performed comparing the nuclear and cytosolic signal. The quantification indeed shows that there is a significant decrease in nuclear RHEB after hatching (figure 11b). Thus, in both medaka and zebrafish, RHEB is present in the nucleus in the embryonic stage, then a strong decrease in nuclear RHEB occurs around hatching.

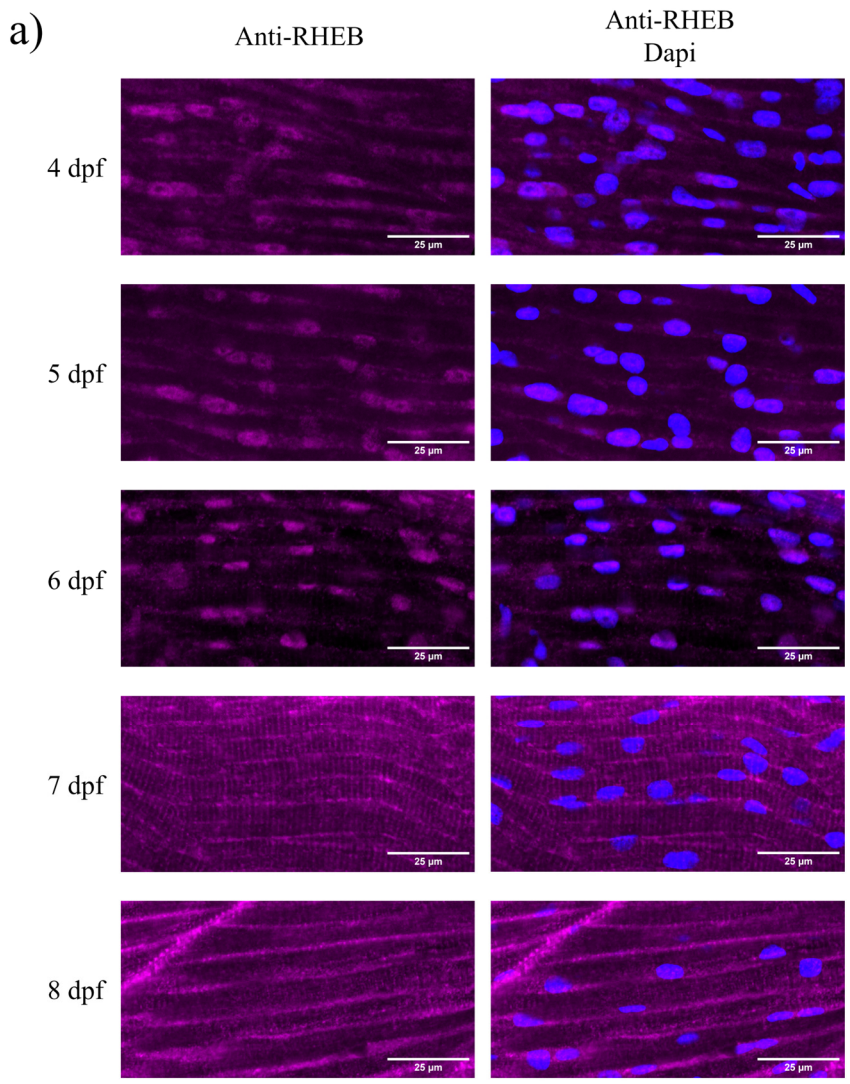

Part **b** and figure legend on next page.

b)

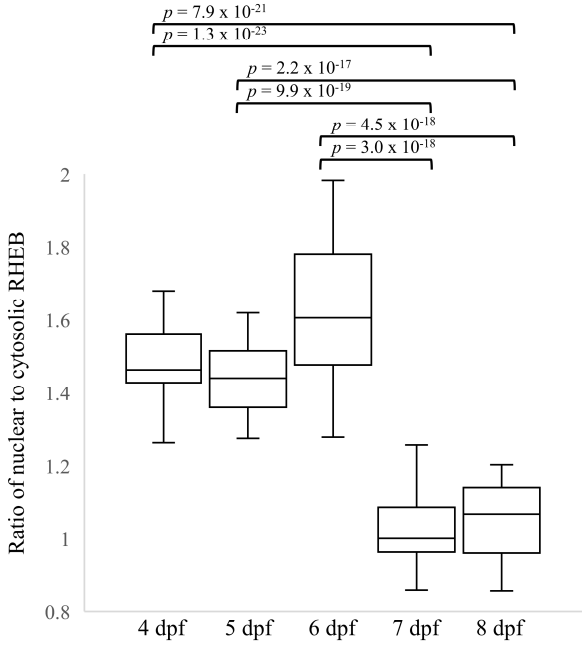

Figure 11: Subcellular localisation of RHEB during Medaka muscle development

Medaka embryo at 4 dpf, 5 dpf and 6 dpf and larvae at 7 dpf and 8 dpf were subjected to wholemount immunofluorescent analysis using an antibody against RHEB (magenta). DAPI was used for counterstaining of the nuclei (blue). **a)** Representative confocal microscopy images are shown (scale bar: 25 µm). **b)** The ratio of the mean signal intensity of RHEB in nuclei (nuclear signal normalized to nucleic surface area) to the mean signal intensity in the cytosol (cytosolic signal normalized to cytosolic surface area) is presented as a box and whiskers plot. For each group at least 30 single myofibres from at least 7 animals (the exception being 8 dpf with 27 myofibres from 6 animals) were analyzed. Bonferroni adjusted α: $p<0.01$.

3.1.3. Localisation of RHEB in the eye during zebrafish development

The reduction of nuclear RHEB in myofibres around the timepoint of hatching raised the question of whether this is also occurring in other cell types. I investigated the localisation of RHEB in the eye of zebrafish. The eye was chosen due to the clarity of the structure during early developmental stages. At 16 hpf RHEB was present in the nucleus, with an enrichment in the nucleolus (figure 12). At 24 hpf there was a slight reduction of nuclear RHEB, a strong signal still being in the nucleolus in the nucleolus. Finally, at 48 hpf there was a strong reduction in nuclear RHEB (preliminary results, as images represent two

fish). This suggests that in the developing eye RHEB is also present in the nucleus at early stages. However, the reduction of nuclear RHEB in the eye occurs before hatching, i.e. earlier than in myofibres.

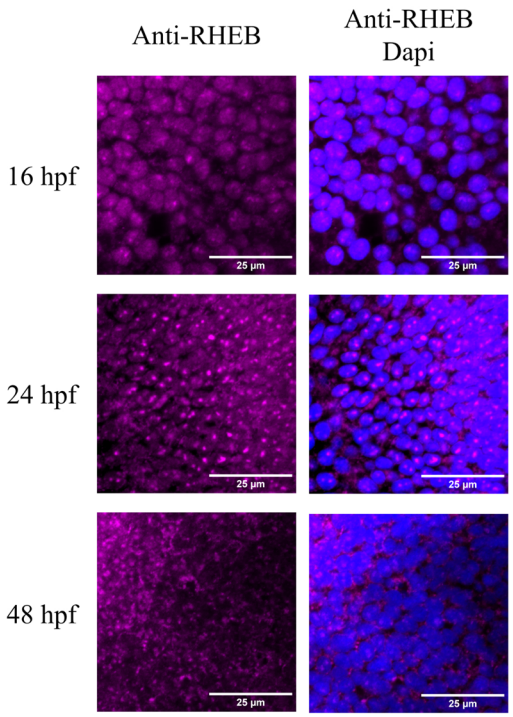

Figure 12: Subcellular localisation of RHEB during zebrafish eye development

Zebrafish embryo at 16 hpf, 24 hpf and 48 hpf were subjected to wholemount immunofluorescent analysis using an antibody against RHEB (magenta). DAPI was used for counterstaining of the nuclei (blue). The presented confocal microscopy images of the eye are representative of 7 animals at 16 hpf and 24 hpf and of 2 animals at 48 hpf (scale bar: 25 µm).

All in all, these results show that RHEB is present in the nucleus during the early developmental stages of the teleost zebrafish and medaka. Nuclear RHEB is reduced during development, the timing of these changes in subcellular localisation being cell type specific.

3.2. Role of muscle activity on RHEB localisation

In zebrafish embryo random twitching can occur after 17 hpf (Saint-Amant & Drapeau, 1998). While this represents the first muscle activity in the embryo the overall muscle movement is very low. In preparation for hatching, muscle activity considerably increases in zebrafish embryo starting at around 60 hpf. This is due to rapid movement being necessary for the process (Kimmel et al., 1995). Finally, in the larval stage the embryo can freely swim and overall muscle activity and movement is increased. Given that the

presence of RHEB in myofibre nuclei strongly decreases around hatching and that hatching is associated with a change in skeletal muscle activity, I investigated the effect both decreased and increased muscle activity has on RHEB subcellular localisation in zebrafish myofibres. Several approaches for reducing muscle activity were utilized: genetic mutation, genetic manipulation and pharmacological treatment.

3.2.1. Effect of motility mutants on RHEB localisation

In a first approach, I used the *steif/unc-45b* zebrafish mutant which show a total lack of movement (Etard et al., 2007). This mutation is in the gene for the unc-45b protein, which is responsible for the folding of the myosin filament in sarcomeres (Barral et al., 2002). Homozygous (-/-) *steif* mutants do not produce functional unc-45b, resulting in disorganized myofibrils and thus leading to paralyzed zebrafish embryos. Due to the lethality of this mutation this mutant can only be used at early developmental stages. For the experiments the embryos were carefully sorted to ensure that indeed homozygous (-/-) *steif* mutants were chosen, based on the absence of random twitching, movement and touch response. At 3 dpf the structure of the muscle in the mutant was totally disorganized (figure 13). For example, while in the control (heterozygous (+/-) and homozygous (+/+) siblings) (figure 13) the z-band was visible (as also before in figure 9a at 2 and 3 dpf), it was not in the homozygous *steif* mutants (figure 13). In the *steif* mutants RHEB was still present in the nuclei of myofibres at 3 dpf, while it had decreased in the control fish. Thus, preventing muscle activity via the mutation of unc-45b results in a prolonged nuclear localisation of RHEB in these mutants. Due to the structural deficiencies in the muscle a quantification of RHEB immunoreactivity in the nuclei and cytosol of single myofibres was not possible.

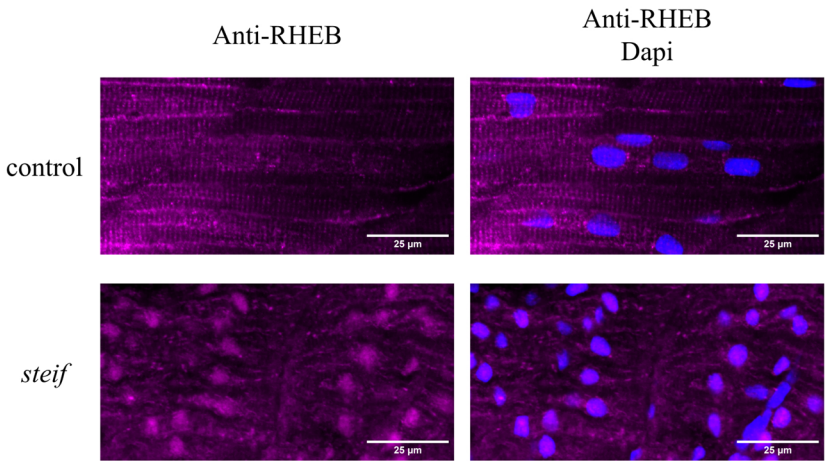

Figure 13: Subcellular localisation of RHEB in *steif* mutants at 3 dpf

Control (heterozygous (+/-) and homozygous (+/+)) and homozygous (-/-) *steif* mutant zebrafish larvae at 3 dpf were subjected to a wholemount immunofluorescent analysis using an antibody against RHEB (magenta). DAPI was used for counterstaining of the nuclei (blue). Images of the muscle acquired by confocal microscopy are representative of at least 7 animals of each genotype (scale bar: 25 µm). (7 no steif 10+ steif)

The *steif* mutation clearly inhibits the decrease in nuclear RHEB at 3 dpf. However, due to the severe disorganization of the myofibres in this mutant, it is not clear whether this effect is caused only by the lack of muscle activity. For further clarification, I used a different mutation, the *sop*^{fixe} or *fixe* mutation (Etard et al., 2005), which also prevents muscle activity. Homozygous (-/-) *fixe* mutants lack clusters of nicotinic acetylcholine receptors, thereby preventing the neurotransmission from motoneurons to myofibres, resulting in a paralysis of the animal. The homozygous (-/-) *fixe* mutants were sorted by checking for a lack of random twitching, movement and touch response. Unlike the *steif* mutants the *fixe* mutants show no disorganisation of the myofibres. The *fixe* mutants also show a retention of RHEB in myonuclei at 3 dpf (figure 14a), as compared to control (heterozygous (+/-) and homozygous (+/+)) larvae. As the *fixe* mutation does not damage the muscle and myofibre structure a quantification was possible. This quantification (figure 14b) confirms that the difference in nuclear RHEB between the paralysed homozygous *fixe* and the moving control larvae is indeed significant. Thus, preventing muscle activity prolongs the localisation of RHEB in the nucleus.

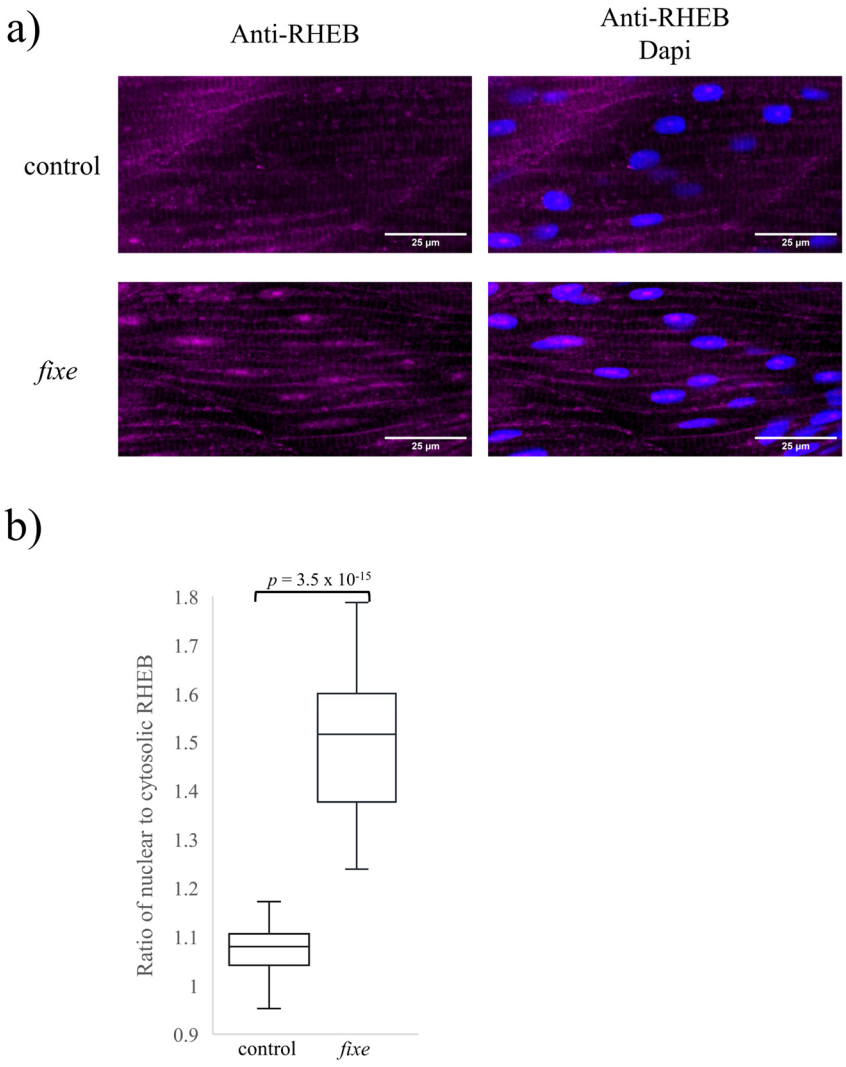

Figure 14: Subcellular localisation of RHEB in *fixe* mutants at 3 dpf

Control (heterozygous (+/-) and homozygous (+/+)) and homozygous (-/-) *fixe* zebrafish larvae at 3 dpf were subjected to a wholemount immunofluorescent analysis using an antibody against RHEB (magenta). DAPI was used for counterstaining of the nuclei (blue). **a)** Images of the muscle acquired by confocal microscopy are representative of at least 7 animals of each genotype (scale bar: 25 µm). **b**) The ratio of the mean signal intensity of RHEB in nuclei (nuclear signal normalized to nucleic surface area) to the mean signal intensity in the cytosol (cytosolic signal normalized to cytosolic surface area) is presented as a box and whiskers plot. For each group at least 30 single myofibres from at least 7 animals were analyzed.

While my results obtained with the *steif* and *fixe* mutants provide a good indication that preventing muscle activity results in a prolonged retention of RHEB in the nucleus, both experiments were dependent on a mutation which could affect other aspects of zebrafish muscle development. Therefore, I complemented these results by using two other approaches to immobilize zebrafish independently of a mutation.

3.2.2. Effect of α-Bungarotoxin on RHEB localisation

In the first approach, I used α-Bungarotoxin which has been shown to be ideal for prolonged immobilization of zebrafish embryos (Swinburne et al., 2015). α-Bungarotoxin is a neurotoxin from the venom of the Southeast Asian banded krait which immobilizes the muscles in a similar way to the *fixe* mutant. It binds with very high affinity to the acetylcholine binding sites of the nicotinic acetylcholine receptor (Tzartos & Changeux, 1983), thereby preventing all skeletal muscle activity. After α-Bungarotoxin mRNA injection, the immobilized embryos were selected based on the absence of random twitching, movement or touch response. Similar to the *fixe* mutants (figure 14a) these embryos showed no apparent disorganization of the myofibre and muscle structure (figure 15a). At 3 dpf, α-Bungarotoxin injected larvae showed a significant nuclear retention of RHEB, as compared to un-injected larvae (figure 15) thus confirming the results obtained with the *fixe* mutant.

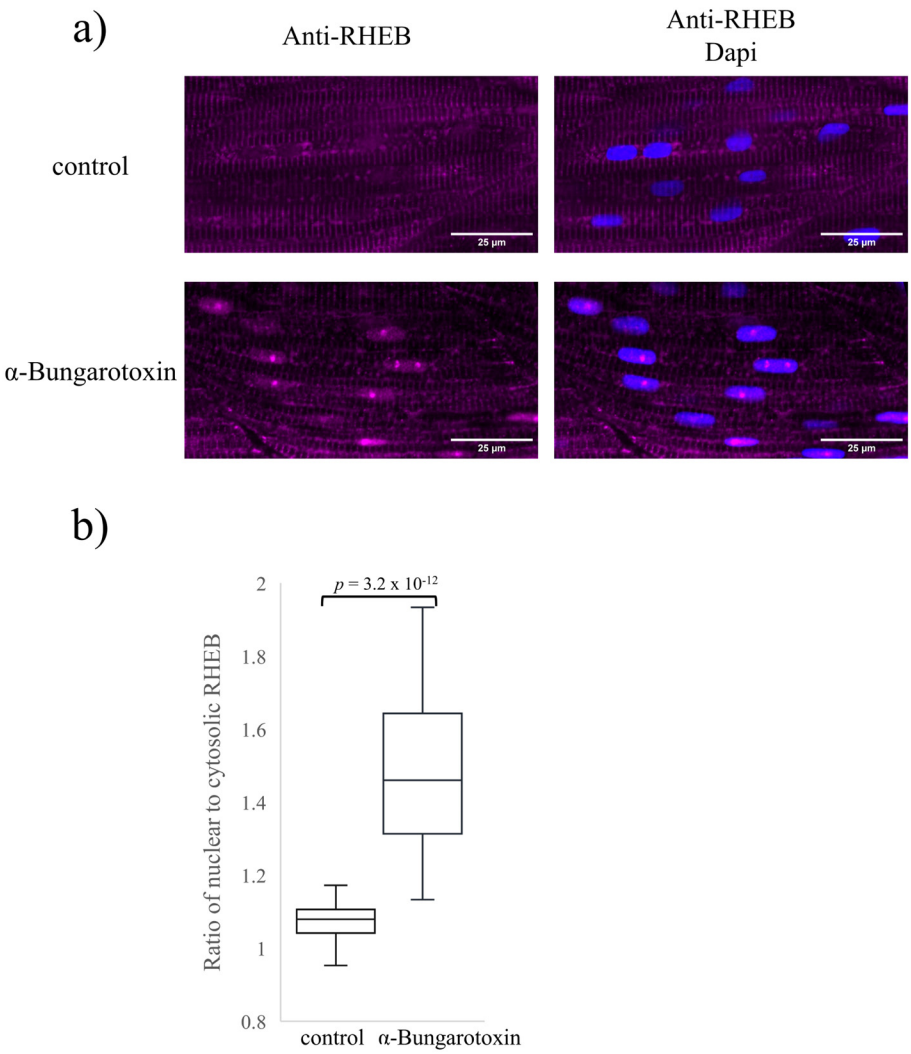

Figure 15: Subcellular localisation of RHEB in zebrafish injected with α-Bungarotoxin

Single cell stage zebrafish embryos were injected (or not injected) with α-Bungarotoxin. At 3 dpf the zebrafish larvae were subjected to a wholemount immunofluorescent analysis using antibodies against RHEB (magenta). DAPI was used for counterstaining of the nuclei (blue). **a)** Representative confocal microscopy images of the muscle are shown (scale bar: 25 µm). **b**) The ratio of the mean signal intensity of RHEB in nuclei (nuclear signal normalized to nucleic surface area) to the mean signal intensity in the cytosol (cytosolic signal normalized to cytosolic surface area) is presented as a box and whiskers plot. For each group at least 30 single myofibres from at least 7 animals were analyzed.

3.2.3. Effect of tricaine on RHEB localisation

In the previous experiments in which I used paralyzed mutants and α-Bungarotoxin mRNA injection, I observed a clear nuclear retention of RHEB at 3 dpf. However, I cannot formally exclude that this effect is an indirect consequence of the manipulation at the very onset of embryonic development. For this reason, I also used a pharmacological approach to immobilize embryos at a time point when skeletal muscle shows spontaneous activity (Saint-Amant & Drapeau, 1998). To this end, I treated 1 dpf zebrafish embryos with tricaine, a widely used anesthetic which immobilizes zebrafish by blocking voltage-gated sodium channels (Attili & Hughes, 2014). Two days of treatment with tricaine resulted in a significant nuclear retention of RHEB at 3 dpf, as compared to untreated animals (figure 16).

Together these experiments confirm that preventing muscle activity in zebrafish embryo results in a prolonged nuclear localisation of RHEB in zebrafish larvae.

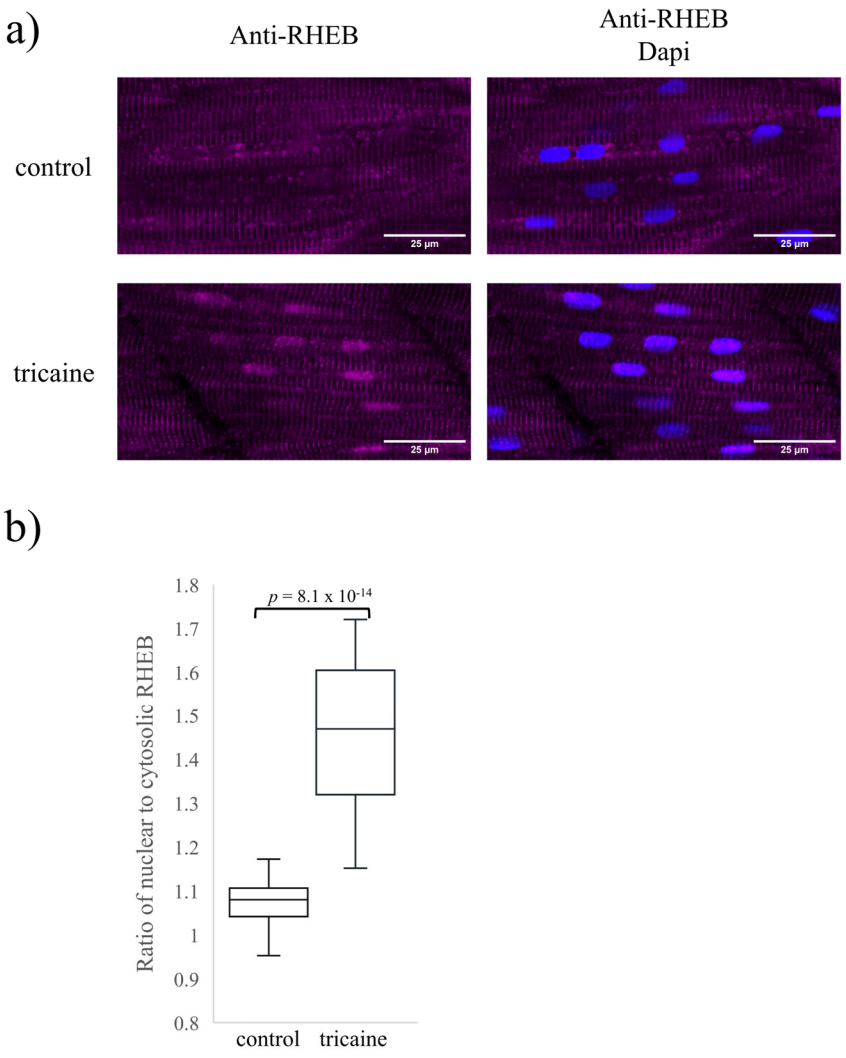

Figure 16: Subcellular localisation of RHEB in tricaine treated zebrafish larvae

Zebrafish embryos were either untreated or anesthetized with tricaine at 1 dpf and then subjected to a wholemount immunofluorescent analysis using an antibody against RHEB (magenta) at 3 dpf. DAPI was used for counterstaining of the nuclei (blue). **a)** Representative confocal microscopy images of the muscles are shown. **b**) The ratio of the mean signal intensity of RHEB in nuclei (nuclear signal normalized against nuclei area) to the mean signal intensity in the cytosol (cytosolic signal normalized against cytosol area) is presented as a box and whiskers plot. For each group at least 30 single myofibres from at least 7 animals were analyzed.

3.2.4. Effect of electrical pulse stimulation on RHEB localisation

My results show that inhibiting muscle activity inhibits the decrease in nuclear RHEB which occurs around the time of hatching. If indeed the increase in muscle activity which occurs around the hatching time is the trigger for the loss of nuclear RHEB, then increasing muscle activity before that time point might result in an earlier reduction of nuclear RHEB. Increasing muscle activity in adult zebrafish is commonly done through swimming exercise models (Palstra et al., 2010; Palstra et al., 2014; Pelster et al., 2003). These systems are clearly not applicable in unhatched embryos, which are not yet freely swimming. For this reason, I adapted a recently described electrical pulse stimulation (EPS) system (Kilroy et al., 2022). The EPS protocol started at 17 hpf, when embryonic myofibre contraction is possible (Saint-Amant & Drapeau, 1998) and ended at 2 dpf, a time point when RHEB is still in the nucleus (see figure 9a at 2 dpf above). Muscles of control embryos raised in the same conditions in the stimulation chambers but without applying EPS showed myonuclear RHEB (figure 17a) and were indistinguishable from the muscles of 2 dpf embryos raised in standard conditions (see figure 9a above). However, in myofibres of EPS treated embryos there was less nuclear RHEB than in the control myofibres (figure 17a). Moreover, the subcellular localisation of RHEB in the EPS treated 2 dpf myofibres was similar to that in untreated wildtype 3 dpf larvae (see figure 9a above). Indeed, the quantification showed a significant difference between EPS treated embryos and untreated (figure 17b). Thus, increasing muscle activity in the embryo prior to hatching accelerates the decrease in nuclear RHEB in myofibres.

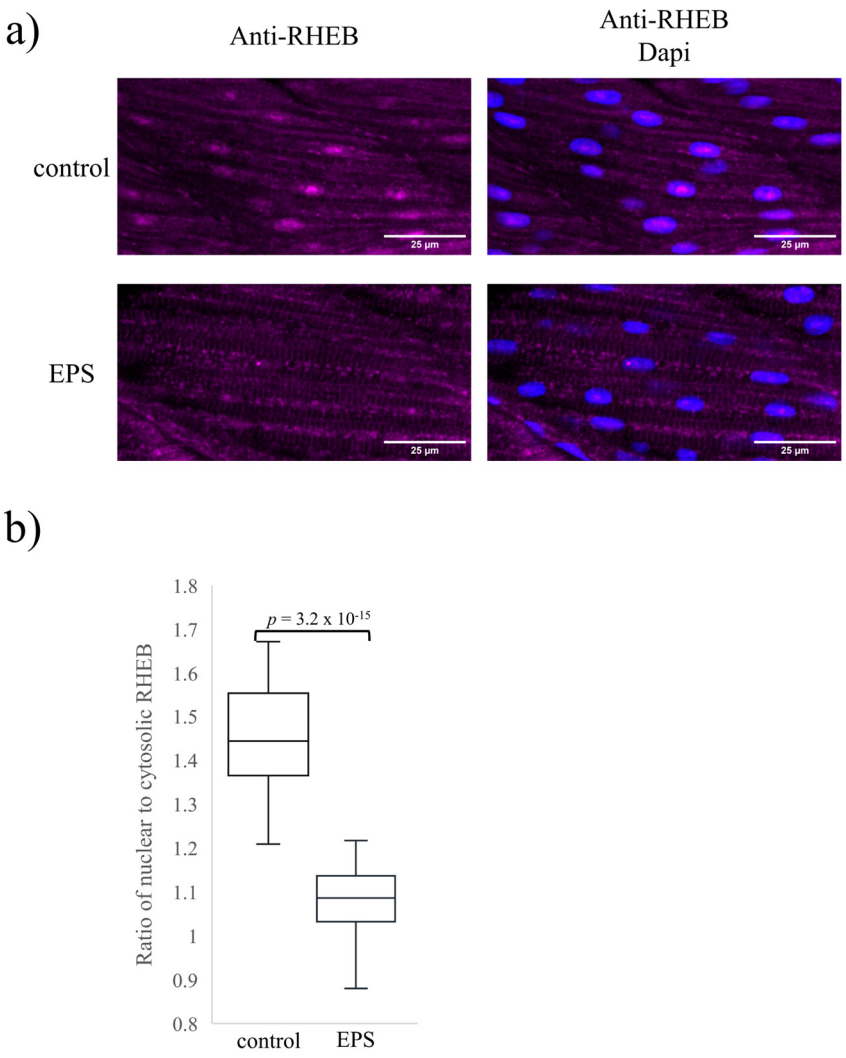

Figure 17: Subcellular localisation of RHEB after electrical pulse stimulation

Zebrafish embryos were either unstimulated or subjected to trains of electric pulses (10 ms, 7 V, 10 Hz) separated by 8 h recovery periods from 17 to 48 hpf. The embryos were then subjected to wholemount immunofluorescent analysis using an antibody against RHEB (magenta). DAPI was used for counterstaining of the nuclei (blue). **a)** Representative confocal microscopy images of the muscle are shown. **b**) The ratio of the mean signal intensity of RHEB in nuclei (nuclear signal normalized against nucleic surface area) to the mean signal intensity in the cytosol (cytosolic signal normalized against cytosolic surface area) is presented as a box and whiskers plot. For each group at least 30 single myofibres from at least 7 animals were analyzed.

3.3. Role of farnesylation on the localisation of RHEB

Together, my results show that in early embryonic myofibres RHEB is strongly localised to the myonuclei, and then progressively leaves the nucleus around hatching time, in a muscle activity-dependent manner. A major determinant of RHEB subcellular localisation is the farnesylation of its C-terminal CAAX motif. Indeed, farnesylation is responsible for the cytosolic retention of RHEB (Angarola & Ferguson, 2019; Buerger et al., 2006; Hanker et al., 2010; Sancak et al., 2008), while inhibiting farnesylation in mammalian cells in culture results in the nuclear accumulation of RHEB (Hanker et al., 2010; Norizadeh Abbariki, 2021). Therefore, a logical hypothesis is that farnesylation is involved in the regulation of RHEB subcellular localisation in zebrafish embryonic myofibres, in particular in the decrease in nuclear RHEB around the time of hatching. To test this hypothesis, I treated 15 hpf zebrafish embryos with the farnesyltransferase inhibitor (FTI) lonafarnib until 3 dpf. Nuclear RHEB had strongly decreased in myofibres from control 3 dpf embryos (figure 18a, see also figure 9a above), whereas it was still present at high levels in the myonuclei from FTI treated embryos (figure 18a & 18b).

These results strongly suggest that preventing the farnesylation of RHEB promotes its nuclear retention in the myofibres of post-hatching zebrafish larvae.

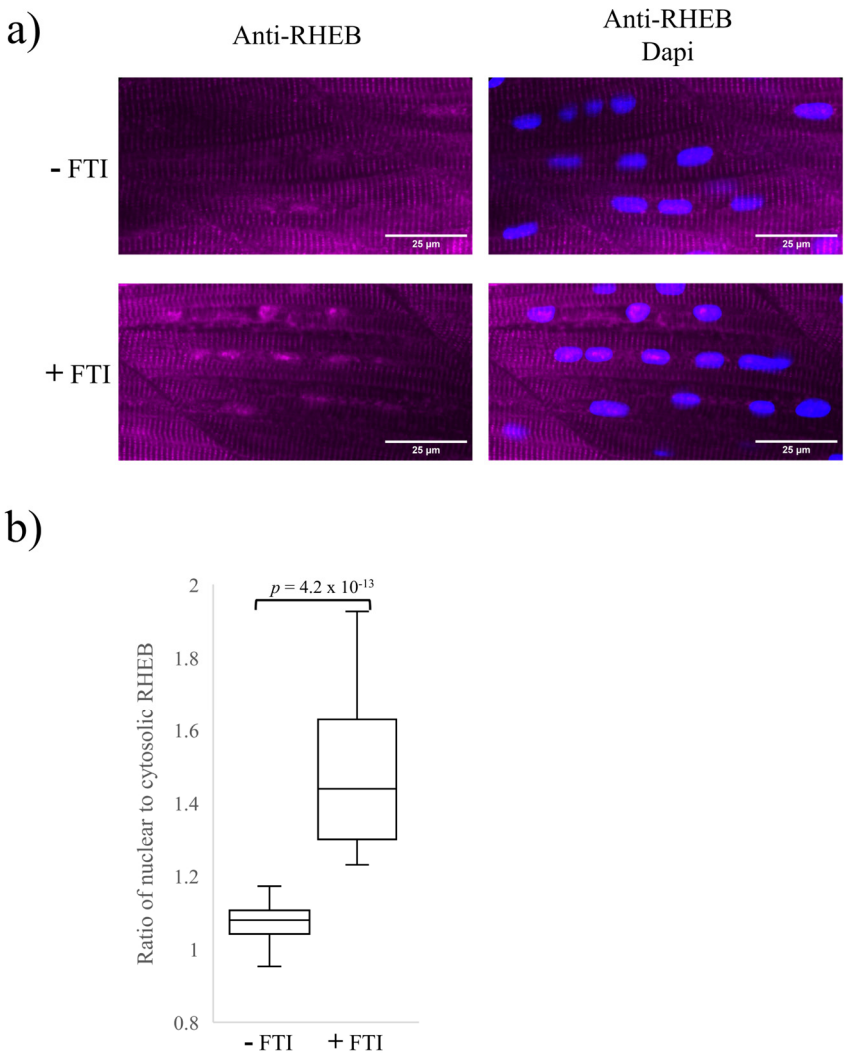

Figure 18: Subcellular localisation of RHEB in FTI treated zebrafish larvae

Zebrafish embryos were either untreated or treated with the farnesyltransferase inhibitor (FTI) at 1 dpf and then subjected to a wholemount immunofluorescent analysis using an antibody against RHEB (magenta) at 3dpf. DAPI was used for counterstaining of the nuclei (blue). **a)** Representative confocal microscopy images of the muscles are shown. **b**) The ratio of the mean signal intensity of RHEB in nuclei (nuclear signal normalized against nuclei area) to the mean signal intensity in the cytosol (cytosolic signal normalized against cytosol area) is presented as a box and whiskers plot. For each group at least 30 single myofibres from at least 7 animals were analyzed.

4. Discussion

In this work, I have investigated the regulation of RHEB subcellular localisation in the myofibres of zebrafish during early development. I show that RHEB is present in the nucleus before hatching and progressively decreases after. This change in subcellular localisation depends on muscle activity and requires RHEB farnesylation.

4.1. Subcellular localisation of RHEB

The first significant observation I made is that RHEB is present in the nucleus of myofibres of zebrafish embryos at 1 and 2 dpf. This nuclear presence of RHEB is strongly reduced at 3 dpf. RHEB has been shown to localise to endomembranes such as those of the lysosome, Golgi and endoplasmic reticulum (Angarola & Ferguson, 2019; Buerger et al., 2006; Hanker et al., 2010; Sancak et al., 2008). However, in several mammalian cell lines RHEB has also been shown to be present in the nucleus (Yadav et al., 2013; Zhong et al., 2022). In zebrafish less is known about the subcellular localisation of RHEB. However, previous results from the laboratory showed that RHEB is also nuclear at 2 dpf in zebrafish myofibres, while being exclusively cytosolic in adult zebrafish myofibres (Norizadeh Abbariki, 2021). I was also able to show that RHEB is not detected in the cytosol of myofibres at 1 dpf. Previous results showed that blocking the cytosolic function of RHEB through the use of a dominant negative RHEB mutant targeted to the cytosol (RHEB-D60K-NES) resulted in a significant reduction in myofibre size at 2 dpf (Norizadeh Abbariki, 2021). Thus, RHEB is present, and necessary in myofibre cytosol at these early stages. These results strongly suggest that the anti-RHEB antibody which I used in the wholemount immunofluorescent staining very weakly recognizes zebrafish cytosolic RHEB. Interestingly, this antibody has been shown to preferably bind to non-farnesylated RHEB (Sugiura et al., 2022), which may explain the weak cytosolic signal, given that cytosolic RHEB is farnesylated (Buerger et al., 2006; Sancak et al., 2008). This interpretation is further supported by my results showing that inhibition of farnesylation results in the retention of RHEB in myonuclei (see also discussion of farnesylation below).

My results also show a strong enrichment of RHEB immunoreactivity in myofibre nucleoli. This enrichment in some cases persisted after 3dpf while immunoreactivity was very strongly reduced in the myonuclei. Knocking down RHEB expression using a morpholino oligonucleotide strongly reduced both the cytosolic and nuclear staining. It had only a weak effect on the nucleolar staining. These results might suggest an increased stability of RHEB in the nucleolus. However, RHEB nucleolar enrichment was not detected in medaka myofibres, strongly suggesting that the antibody recognizes another epitope on a zebrafish nucleolar protein.

Furthermore, both in zebrafish and medaka myofibres, once cytosolic RHEB becomes more prevalent it localises predominantly along the z-line of the sarcomere. While it is possible that this is an artefact due to antibody entrapment, it may also reflect the localisation to internal membranes. In myofibres the lysosome, which is a described localisation of RHEB (Angarola & Ferguson, 2019; Parmar & Tamanoi, 2010; Sancak et al., 2008), is present throughout the cytosol and not located around the z-line (Douillard-Guilloux et al., 2010; Steen et al., 2009). Nonetheless, RHEB has been shown to localise at other structures, including the Golgi, endoplasmic reticulum (ER), mitochondria and autophagosome (Angarola & Ferguson, 2019; Dengjel et al., 2012; Hanker et al., 2010; Melser et al., 2013; Yang et al., 2021). In myofibres, these structures can be localised at the myofibrils and around the z-line (Douillard-Guilloux et al., 2010; Leduc-Gaudet et al., 2023; Ogata & Yamasaki, 1987; Walker & Edge, 1971; Xiao et al., 2015). Thus, cytosolic RHEB may localise around the z-line due to the endomembrane structures in myofibres.

Together, this shows that before 3 dpf, RHEB is present both in the cytosol and nucleus of myofibres and is then progressively reduced in the nucleus after 3 dpf.

4.2. Regulation of RHEB nuclear localisation

The time at which I observed a decrease in RHEB presence in the nucleus of zebrafish myofibres corresponds to hatching. Indeed, in zebrafish the timepoint of hatching, when the embryos emerge from the chorion and are classified as larvae, is between 2 and 3

dpf (Kimmel et al., 1995). I confirmed this result using medaka as another fish model. I showed that in medaka myofibres RHEB is nuclear during the first 6 dpf and that there is a reduction in nuclear RHEB at 7 dpf. Zebrafish and medaka are both teleost fish which, while similar in size, anatomy and physiology, are only distantly related. The development of the two fish differs, medaka developing significantly slower. Zebrafish embryo segmentation starts at around 10 hpf with the 1-4 somite stage and ends at around 24 hpf (Kimmel et al., 1995). In medaka it only starts at around 27 hpf and ends at around 101 hpf (Iwamatsu, 2004). In medaka hatching takes place between 6 and 7 dpf (under our incubation conditions). My results show that in myofibres of two different teleost fish RHEB is present in the nucleus of myofibres of embryos and, after hatching there is a reduction of nuclear RHEB in the myofibre of the larvae.

What could be the mechanism of RHEB relocalisation at the time of hatching? A major change occurring in zebrafish muscle around the time of this process is muscle activity. During early zebrafish development, after 17 hpf, random twitching can occur, this being the first muscle activity of the zebrafish (Saint-Amant & Drapeau, 1998). However, the overall movement and muscle activity is very low. During the process of hatching (starting at ~60 hpf) rapid movement is necessary (Kimmel et al., 1995) and after hatching the larvae can swim freely and overall muscle activity is greatly increased. The zebrafish myofibres after hatching are fully differentiated and have a functional sarcomere structure that can fully contract. This leads to a visible striation of the myofibre as well as multiple myonuclei with a peripheral localisation. These are all indications of fully differentiated mature myofibres at the larval stage. Furthermore, at 72 hpf there is an increase in muscle hypertrophy and hyperplasia, the first pax7-expressing muscle stem cells arise and the zebrafish myotome expands giving rise to the secondary myotome (Hollway et al., 2007; Rowlerson & Veggetti, 2001; Seger et al., 2011; Stellabotte et al., 2007).

My findings are that indeed muscle activity can influence the nuclear localisation of RHEB in zebrafish embryo myofibres. Reducing or preventing muscle activity through the use of genetic models (*steif* mutant and *fixe* mutant), genetic manipulation (injection of α-Bungarotoxin mRNA) or pharmaceuticals (tricaine), resulted in a longer presence of RHEB in the nucleus. RHEB was still present in the nucleus of myofibres at 3 dpf, while

there was a strong reduction in untreated wildtype fish. Furthermore, increasing muscle activity through the use of electrical pulse stimulation resulted in the reduction of nuclear RHEB occurring earlier, at 2 dpf.

Whether muscle contraction itself regulates the presence of RHEB in the nucleus is still unclear. Another possibility is that the reduction in nuclear RHEB occurring after hatching in the larval stage is the result of myofibre maturation. Indeed, there are indications that muscle activity promotes myofibre maturation. Exercise has been shown to promote production of transcription factors necessary for differentiation and to affect muscle remodeling (Ferraro et al., 2014). It has also been shown that mice with advanced endurance exercise performance showed increases in myogenic markers, functionality and differentiation (Petkov et al., 2022). Finally, electrical pulse stimulation, which I used to increase muscle activity in the zebrafish embryo, has been shown to accelerate myotube maturation (Fujita et al., 2007). Furthermore, preliminary results from the laboratory suggest that electrical pulse stimulation increases myofibre maturation *in vitro* in C2C12 mouse myoblasts and affects RHEB subcellular localisation. Therefore, it seems likely that RHEB is excluded from the myonucleus as a result of myofibre maturation.

My results also suggest that this mechanism is not restricted to myofibre maturation. I show that in cells of the zebrafish eye RHEB is strongly present in the nucleus at 18 hpf and 24 hpf. My preliminary results also suggest that this is followed by a strong reduction in nuclear RHEB at 48 hpf, an early timepoint compared to the decreased RHEB presence in myonuclei. The cells of the zebrafish eye develop differently from myofibres and are consequently not dependent on muscle activity and hatching. During the first 28 hours post fertilization there is a rapid development of the eye in the zebrafish embryo, from an early formation of the optic lumina at 14 hpf to detachment of the lens mass at 28 hpf (Richardson et al., 2017). Thus, the differentiation and maturation of the zebrafish eye seems to also be accompanied by a decrease in nuclear RHEB, suggesting that this regulation of RHEB nuclear localisation might be a general developmental process.

4.3. Role of farnesylation in the regulation of RHEB localisation

My results show that preventing farnesylation in zebrafish embryo, through the use of a farnesyl transferase inhibitor, results in the retention of RHEB in myonuclei at 3 dpf, a time point at which RHEB was excluded from the myonuclei in the untreated embryo. The C-terminal farnesylation of RHEB, which is achieved through the addition of a farnesyl group to the C-terminal CAAX motif of RHEB, promotes the localisation and attachment of RHEB to internal membranes (Buerger et al., 2006).

While other members of the Ras family are also farnesylated, there are further mechanisms which cooperate with farnesylation to target them to the plasma membrane. Both H-Ras and K-Ras-4B have palmitoylated cysteines, additionally K-Ras-4B has polybasic regions (Hancock et al., 1990; Takahashi et al., 2005; Zhou & Hancock, 2018). RHEB however, does not harbor additional targeting signals and is only loosely targeted to internal membranes via farnesylation (Ferguson & Angarola, 2020).

Thus, it is unclear if the nuclear form of RHEB is farnesylated. Recent studies have shown that preventing farnesylation of RHEB by inhibiting farnesyltransferase activity in mammalian cells *in vitro* leads to an accumulation of RHEB in the nucleus (Hanker et al., 2010). My experiments corroborate these findings, however taking place *in vivo* in zebrafish embryos. These results suggest an involvement of farnesylation in the retention of RHEB in the cytosol. The mechanism behind nuclear localisation of RHEB is not yet understood. A possibility is diffusion into the nucleus through nuclear pores due to the small size of RHEB (21 kDa). Thus, cytosolic localisation could be due to accumulation and retention at endomembranes via farnesylation, whereas nuclear localisation could be due accumulation and retention in the nucleus. While the mechanism behind the nuclear retention is not yet known, a possibility could be an interaction with proteins residing in the nucleus.

An indication that nuclear RHEB may not be farnesylated comes from the relative levels of nuclear and cytosolic RHEB in myofibres during the first day of zebrafish development. The RHEB antibody that I used recognizes both the farnesylated and non-farnesylated form of RHEB, with a demonstrated preference for binding to the non-farnesylated form

(Sugiura et al., 2022). The almost undetectable RHEB immunoreactivity in the cytosol at 1 dpf, even though RHEB is present in the cytosol at this stage (see above), together with the strong immunoreactivity in the nucleus may indicate that indeed cytosolic RHEB is farnesylated, while nuclear RHEB is not and thereby efficiently recognized by the antibody. My observation that farnesyltransferase activity is required for the decrease in nuclear RHEB at the time of hatching also strongly suggests that nuclear RHEB is not farnesylated.

A corollary is that RHEB farnesylation is somehow regulated. A general regulation of farnesyltransferase expression or activity is rather unlikely. Indeed, members of the Ras family of proteins are mostly farnesylated (Kho et al., 2004). For example, K-Ras is required during early zebrafish development (Liu et al., 2008). However, while K-Ras is generally farnesylated (Kho et al., 2004; Takahashi et al., 2005) it has been shown that blocking farnesylation leads to a geranylgeranylation (a different prenylation) of K-Ras (Whyte et al., 1997). Nevertheless, a regulation of the expression or activity of farnesyltransferase seems unlikely as the regulatory mechanism behind the regulation of RHEB subcellular localisation.

Thus, before hatching there might be two pools of RHEB, one farnesylated and localised in the cytosol, and one not farnesylated and accumulating in the myonucleus. At time of hatching all newly expressed RHEB would be farnesylated and retained in the cytosol, with as a consequence a progressive decrease in nuclear RHEB.

4.4. Putative function of nuclear RHEB in embryonic myofibres

Previous results of the laboratory have shown that in zebrafish embryonic myofibres nuclear RHEB promotes myofibre growth (Norizadeh Abbariki, 2021). The mechanism behind such an effect remains as of yet unknown. The mechanism of such an effect remains unknown.

One possibility is the activation of mTORC1 in the nucleus. Indeed, mTORC1 activity is a strong driver of muscle growth (Bodine, 2022; Bodine et al., 2001; Schiaffino &

Mammucari, 2011; You et al., 2019), and nuclear RHEB has been shown to activate nuclear mTORC1 (Zhong et al., 2022). However, the myofibre growth-promoting effect of nuclear RHEB has been shown to be mTORC1-independent (Norizadeh Abbariki, 2021).

RHEB has been shown to regulate several signalling pathways in an mTORC1-independent manner (Karbowniczek et al., 2006; Karbowniczek et al., 2010; Lacher et al., 2010; Meng et al., 2019; Norizadeh Abbariki, 2021; Sato et al., 2015). Interestingly, some of these regulations might take place in the nucleus. Among these are the AMPK and the Notch signalling pathway (Karbowniczek et al., 2010; Lacher et al., 2010; Meng et al., 2019).

RHEB has been shown to interact with AMPK and activate it in the cytosol in an mTORC1 independent manner (Lacher et al., 2010). Furthermore, AMPK has been shown to be present in the nucleus (McGee et al., 2003) and has been shown to be involved in energy delivery to the muscle especially in response to stress (O'Neill et al., 2011; Zong et al., 2002). This prompts the speculation that RHEB could also activate AMPK in the nucleus in an mTORC1 independent manner. However, AMPK has been shown to upregulate muscle degradation and inhibit muscle growth (Mounier et al., 2009; Nakashima & Yakabe, 2007; Sanchez et al., 2012; Williamson et al., 2009) while nuclear RHEB promotes myofibre growth.

RHEB has also been reported to interact with Notch in an mTOR-independent manner (Karbowniczek et al., 2010; Meng et al., 2019). For example, RHEB has shown to activate Notch in an mTOR-independent manner during *Drosophila* development (Karbowniczek et al., 2010). RHEB also helped promote Notch-dependent activation of PKA in brown adipocytes (Meng et al., 2019). Notably, Notch regulates somite differentiation (Jiang et al., 2000; Lewis et al., 2009) and severs a crucial role in the maintenance and growth of skeletal muscles (Al Jaam et al., 2016). Given that upon activation Notch intracellular domain (NICD) is released and translocates to the nucleus, including in myofibres (Bröhl et al., 2012), it is tempting to speculate that RHEB in the nucleus interacts with NICD and regulates the expression of Notch target genes. Such a target gene might be c-Myc which is directly regulated by Notch signalling (Palomero et al., 2006). Interestingly, c-Myc is

present in myonuclei (Veal & Jackson, 1998) and promotes ribosome biogenesis in muscles (Mori et al., 2021), which is a major driver of protein synthesis required for muscle hypertrophy (von Walden et al., 2016).

4.5. Conclusion

In this work I have uncovered a regulation of RHEB subcellular localisation in embryonic myofibres. I propose the existence of two pools of RHEB, one farnesylated and localised to the cytosol, and the other not farnesylated and nuclear. My results showing the role of muscle activity in the decrease in RHEB nuclear localisation around the time of hatching strongly suggest that RHEB subcellular localisation is linked to the maturation of myofibres. Furthermore, I propose that the regulation of RHEB nuclear localisation might be a general mechanism linked to cell differentiation and maturation.

5. References

Abmayr, S.M., & Pavlath, G.K. (**2012**). Myoblast fusion: lessons from flies and mice. *Development*, *139*, 641.

Afinanisa, Q., Cho, M.K., & Seong, H.A. (**2021**). AMPK localization: a key to differential energy regulation. *Int J Mol Sci*, *22*, 10921.

Al Jaam, B., Heu, K., Pennarubia, F., Segelle, A., Magnol, L., Germot, A., Legardinier, S., Blanquet, V., & Maftah, A. (**2016**). Reduced Notch signalling leads to postnatal skeletal muscle hypertrophy in Pofut1cax/cax mice. *Open Biol*, *6*, 160211.

Angarola, B., & Ferguson, S.M. (**2019**). Weak membrane interactions allow Rheb to activate mTORC1 signaling without major lysosome enrichment. *Mol Biol Cell*, *30*, 2750.

Anthony, J.C., Yoshizawa, F., Anthony, T.G., Vary, T.C., Jefferson, L.S., & Kimball, S.R. (**2000**). Leucine stimulates translation initiation in skeletal muscle of postabsorptive rats via a rapamycin-sensitive pathway. *J Nutr*, *130*, 2413–2419.

Attili, S., & Hughes, S.M. (**2014**). Anaesthetic tricaine acts preferentially on neural voltage-gated sodium channels and fails to block directly evoked muscle contraction. *PLoS One*, *9*, e103751.

Bai, X., Ma, D., Liu, A., Shen, X., Wang, Q.J., Liu, Y., & Jiang, Y. (**2007**). Rheb activates mTOR by antagonizing its endogenous inhibitor, FKBP38. *Science*, *318*, 977–980.

Barral, J.M., Hutagalung, A.H., Brinker, A., Hartl, F.U., & Epstein, H.F. (**2002**). Role of the myosin assembly protein UNC-45 as a molecular chaperone for myosin. *Science (1979)*, *295*, 669–671.

Barresi, M.J.F., D'Angelo, J.A., Hernández, L.P., & Devoto, S.H. (**2001**). Distinct mechanisms regulate slow-muscle development. *Curr Biol*, *11*, 1432–1438.

Bentzinger, C.F., Romanino, K., Cloëtta, D., Lin, S., Mascarenhas, J.B., Oliveri, F., Xia, J., Casanova, E., Costa, C.F., Brink, M., Zorzato, F., Hall, M.N., & Rüegg, M.A. (**2008**). Skeletal muscle-specific ablation of raptor, but not of Rictor, causes metabolic changes and results in muscle dystrophy. *Cell Metab*, *8*, 411–424.

Biga, P.R., & Goetz, F.W. (**2006**). Zebrafish and giant danio as models for muscle growth: Determinate vs. indeterminate growth as determined by morphometric analysis. *Am J Physiol Regul Integr Comp Physiol*, *291*, 1327–1337.

Bodine, S.C. (**2022**). The role of mTORC1 in the regulation of skeletal muscle mass. *Fac Rev*, *11*, 11–32.

Bodine, S.C., Stitt, T.N., Gonzalez, M., Kline, W.O., Stover, G.L., Bauerlein, R., Zlotchenko, E., Scrimgeour, A., Lawrence, J.C., Glass, D.J., & Yancopoulos, G.D. (**2001**). Akt/mTOR pathway is a crucial regulator of skeletal muscle hypertrophy and can prevent muscle atrophy in vivo. *Nat Cell Biol*, *3*, 1014–1019.

Bröhl, D., Vasyutina, E., Czajkowski, M.T., Griger, J., Rassek, C., Rahn, H.P., Purfürst, B., Wende, H., & Birchmeier, C. (**2012**). Colonization of the satellite cell niche by skeletal muscle progenitor cells depends on Notch signals. *Dev Cell*, *23*, 469–481.

Buerger, C., DeVries, B., & Stambolic, V. (**2006**). Localization of Rheb to the endomembrane is critical for its signaling function. *Biochem Biophys Res Commun*, *344*, 869–880.

Cafferkey, R., Young, P.R., Mclaughlin, M.M., Bergsma, D.J., Koltin, Y., Sathe, G.M., Faucet1ie, L., Eng, W.-K., Johnson, R.K., & Livi1, G.P. (**1993**). Dominant missense mutations in a novel yeast protein related to mammalian phosphatidylinositol 3-kinase and VPS34 abrogate rapamycin cytotoxicity. *Mol Cell Biol*, *13*, 6012.

Chal, J., & Pourquié, O. (**2017**). Making muscle: skeletal myogenesis in vivo and in vitro. *Development*, *144*, 2104–2122.

Chauvin, C., Koka, V., Nouschi, A., Mieulet, V., Hoareau-Aveilla, C., Dreazen, A., Cagnard, N., Carpentier, W., Kiss, T., Meyuhas, O., & Pende, M. (**2013**). Ribosomal protein S6 kinase activity controls the ribosome biogenesis transcriptional program. *Oncogene*, *33*, 474–483.

Chromiak, J.A., & Antonio, J. (**2008**). Skeletal muscle plasticity. *Essentials of Sports Nutrition and Supplements*, 21–52.

Cossu, G., Angelis, L.D., Borello, U., Berarducci, B., Buffa, V., Sonnino, C., Coletta, M., Vivarelli, E., Marinabouche, '., Lattanzi, L., Tosoni, D., Donna, S.D., Berghella, L., Salvatori, G., Murphy, P., Angelis, M.G.C., & Molinaro, M. (**2000**). Determination, diversification and multipotency of mammalian myogenic cells. *Int J Dev Biol*, *44*, 599–706.

Dengjel, J., Høyer-Hansen, M., Nielsen, M.O., Eisenberg, T., Harder, L.M., Schandorff, S., Farkas, T., Kirkegaard, T., Becker, A.C., Schroeder, S., Vanselow, K., Lundberg, E., Nielsen, M.M., Kristensen, A.R., Akimov, V., Bunkenborg, J., Madeo, F., Jäättelä, M., & Andersen, J.S. (**2012**). Identification of autophagosome-associated proteins and regulators by quantitative proteomic analysis and genetic screens. *Mol Cell Proteomics*, *11*, 1–17.

Devoto, S.H., Melançon, E., Eisen, J.S., & Westerfield, M. (**1996**). Identification of separate slow and fast muscle precursor cells in vivo, prior to somite formation. *Development*, *122*, 3371–3380.

Devoto, S.H., Stoiber, W., Hammond, C.L., Steinbacher, P., Haslett, J.R., Barresi, M.J.F., Patterson, S.E., Adiarte, E.G., & Hughes, S.M. (**2006**). Generality of vertebrate developmental patterns: evidence for a dermomyotome in fish. *Evol Dev*, *8*, 101.

Dorrello, N.V., Peschiaroli, A., Guardavaccaro, D., Colburn, N.H., Sherman, N.E., & Pagano, M. (**2006**). S6K1- and betaTRCP-mediated degradation of PDCD4 promotes protein translation and cell growth. *Science*, *314*, 467–471.

Douillard-Guilloux, G., Raben, N., Takikita, S., Ferry, A., Vignaud, A., Guillet-Deniau, I., Favier, M., Thurberg, B.L., Roach, P.J., Caillaud, C., & Richard, E. (**2010**). Restoration of muscle functionality by genetic suppression of glycogen synthesis in a murine model of Pompe disease. *Hum Mol Genet*, *19*, 684.

Düvel, K., Yecies, J.L., Menon, S., Raman, P., Lipovsky, A.I., Souza, A.L., Triantafellow, E., Ma, Q., Gorski, R., Cleaver, S., Vander Heiden, M.G., MacKeigan, J.P., Finan, P.M., Clish, C.B., Murphy, L.O., & Manning, B.D. (**2010**). Activation of a metabolic gene regulatory network downstream of mTOR complex 1. *Mol Cell*, *39*, 171.

Etard, C., Behra, M., Ertzer, R., Fischer, N., Jesuthasan, S., Blader, P., Geisler, R., & Strähle, U. (**2005**). Mutation in the δ-subunit of the nAChR suppresses the muscle defects caused by lack of Dystrophin. *Dev Dyn*, *234*, 1016–1025.

Etard, C., Behra, M., Fischer, N., Hutcheson, D., Geisler, R., & Strähle, U. (**2007**). The UCS factor Steif/Unc-45b interacts with the heat shock protein Hsp90a during myofibrillogenesis. *Dev Biol*, *308*, 133–143.

Ferguson, S.M., & Angarola, B. (**2020**). Coordination of Rheb lysosomal membrane interactions with mTORC1 activation. *F1000Res*, *9*, Faculty Rev-450.

Ferraro, E., Giammarioli, A.M., Chiandotto, S., Spoletini, I., & Rosano, G. (**2014**). Exercise-induced skeletal muscle remodeling and metabolic adaptation: redox signaling and role of autophagy. *Antioxid Redox Signal*, *21*, 154.

Flück, M., & Hoppeler, H. (**2003**). Molecular basis of skeletal muscle plasticity--from gene to form and function. *Rev Physiol Biochem Pharmacol*, *146*, 159–216.

Frontera, W.R., & Ochala, J. (**2015**). Skeletal muscle: a brief review of structure and function. *Calcif Tissue Int*, *96*, 183–195.

Fujita, H., Nedachi, T., & Kanzaki, M. (**2007**). Accelerated de novo sarcomere assembly by electric pulse stimulation in C2C12 myotubes. *Exp Cell Res*, *313*, 1853–1865.

Furrer, R., Hawley, J.A., & Handschin, C. (**2023**). The molecular athlete: exercise physiology from mechanisms to medals. *Physiol Rev*, *103*, 1693.

Fyfe, J.J., Bishop, D.J., Bartlett, J.D., Hanson, E.D., Anderson, M.J., Garnham, A.P., & Stepto, N.K. (**2018**). Enhanced skeletal muscle ribosome biogenesis, yet attenuated mTORC1 and ribosome biogenesis-related signalling, following short-term concurrent versus single-mode resistance training. *Sci Rep*, *8*, 560.

Geiduschek, E.P., & Tocchini-Valentini, G.P. (**1988**). Transcription by RNA polymerase III. *Annu Rev Biochem*, *57*, 873–914.

Gingras, A.C., Gygi, S.P., Raught, B., Polakiewicz, R.D., Abraham, R.T., Hoekstra, M.F., Aebersold, R., & Sonenberg, N. (**1999**). Regulation of 4E-BP1 phosphorylation: a novel two-step mechanism. *Genes Dev*, *13*, 1422.

Gingras, A.C., Raught, B., & Sonenberg, N. (**1999**). eIF4 initiation factors: effectors of mRNA recruitment to ribosomes and regulators of translation. *Annu Rev Biochem*, *68*, 913–963.

Glass, D.J. (**2003**). Molecular mechanisms modulating muscle mass. *Trends Mol Med*, *9*, 344–350.

Glass, D.J. (**2005**). Skeletal muscle hypertrophy and atrophy signaling pathways. *Int J Biochem Cell Biol*, *37*, 1974–1984.

Goldberg, A.L. (**1969**). Protein turnover in skeletal muscle. *J Biol Chem*, *244*, 3223–3229.

Gonzalez, A.M. (**2016**). Acute anabolic response and muscular adaptation after hypertrophy-style and strength-style resistance exercise. *J Strength Cond Res*, *30*, 2959–2964.

Guertin, D.A., Stevens, D.M., Thoreen, C.C., Burds, A.A., Kalaany, N.Y., Moffat, J., Brown, M., Fitzgerald, K.J., & Sabatini, D.M. (**2006**). Ablation in mice of the

mTORC components Raptor, Rictor, or mLST8 reveals that mTORC2 Is required for signaling to Akt-FOXO and PKCα, but not S6K1. *Dev Cell*, *11*, 859–871.

Haeusler, R.A., & Engelke, D.R. (**2006**). Spatial organization of transcription by RNA polymerase III. *Nucleic Acids Res*, *34*, 4826.

Hancock, J.F., Paterson, H., & Marshall, C.J. (**1990**). A polybasic domain or palmitoylation is required in addition to the CAAX motif to localize p21ras to the plasma membrane. *Cell*, *63*, 133–139.

Hanker, A.B., Mitin, N., Wilder, R.S., Henske, E.P., Tamanoi, F., Cox, A.D., & Der, C.J. (**2010**). Differential requirement of CAAX-mediated posttranslational processing for Rheb localization and signaling. *Oncogene*, *29*, 380–391.

Hara, K., Maruki, Y., Long, X., Yoshino, K. ichi, Oshiro, N., Hidayat, S., Tokunaga, C., Avruch, J., & Yonezawa, K. (**2002**). Raptor, a binding partner of target of rapamycin (TOR), mediates TOR action. *Cell*, *110*, 177–189.

Heard, J.J., & Tamanoi, F. (**2018**). GTP-binding protein Rheb. *Encyclopedia of Signaling Molecules*, 2288–2293.

Henry, C.A., & Amacher, S.L. (**2004**). Zebrafish slow muscle cell migration induces a wave of fast muscle morphogenesis. *Dev Cell*, *7*, 917–923.

Hollway, G.E., Bryson-Richardson, R.J., Berger, S., Cole, N.J., Hall, T.E., & Currie, P.D. (**2007**). Whole-somite rotation generates muscle progenitor cell compartments in the developing zebrafish embryo. *Dev Cell*, *12*, 207–219.

Holz, M.K., Ballif, B.A., Gygi, S.P., & Blenis, J. (**2005**). mTOR and S6K1 mediate assembly of the translation preinitiation complex through dynamic protein interchange and ordered phosphorylation events. *Cell*, *123*, 569–580.

Huang, J., & Manning, B.D. (**2008**). The TSC1–TSC2 complex: a molecular switchboard controlling cell growth. *Biochem J*, *412*, 179.

Huang, J., & Manning, B.D. (**2009**). A complex interplay between Akt, TSC2, and the two mTOR complexes. *Biochem Soc Trans*, *37*, 217.

Huang, S., Bjornsti, M.A., & Houghton, P.J. (**2003**). Rapamycins: mechanisms of action and cellular resistance. *Cancer Biol Ther*, *2*, 222–232.

Huang, S., & Houghton, P.J. (**2001**). Mechanisms of resistance to rapamycins. *Drug Resist Updat*, *4*, 378–391.

Im, E., Von Lintig, F.C., Chen, J., Zhuang, S., Qui, W., Chowdhury, S., Worley, P.F., Boss, G.R., & Pilz, R.B. (**2002**). Rheb is in a high activation state and inhibits B-Raf kinase in mammalian cells. *Oncogene*, *21*, 6356–6365.

Inoki, K., Li, Y., Zhu, T., Wu, J., & Guan, K.L. (**2002**). TSC2 is phosphorylated and inhibited by Akt and suppresses mTOR signalling. *Nat Cell Biol*, *4*, 648–657.

Iwamatsu, T. (**2004**). Stages of normal development in the medaka Oryzias latipes. *Mech Dev*, *121*, 605–618.

Janssen, I., Heymsfield, S.B., Wang, Z.M., & Ross, R. (**2000**). Skeletal muscle mass and distribution in 468 men and women aged 18-88 yr. *J Appl Physiol (1985)*, *89*, 81–88.

Jhanwar-Uniyal, M., Wainwright, J. V., Mohan, A.L., Tobias, M.E., Murali, R., Gandhi, C.D., & Schmidt, M.H. (**2019**). Diverse signaling mechanisms of mTOR complexes: mTORC1 and mTORC2 in forming a formidable relationship. *Adv Biol Regul*, *72*, 51–62.

Jiang, Y.J., Aerne, B.L., Smithers, L., Haddon, C., Ish-Horowicz, D., & Lewis, J. (**2000**). Notch signalling and the synchronization of the somite segmentation clock. *Nature*, *408*, 475–479.

Karbowniczek, M., Robertson, G.P., & Henske, E.P. (**2006**). Rheb inhibits C-Raf activity and B-Raf/C-Raf heterodimerization. *J Biol Chem*, *281*, 25447–25456.

Karbowniczek, M., Zitserman, D., Khabibullin, D., Hartman, T., Yu, J., Morrison, T., Nicolas, E., Squillace, R., Roegiers, F., & Henske, E.P. (**2010**). The evolutionarily conserved TSC/Rheb pathway activates Notch in tuberous sclerosis complex and Drosophila external sensory organ development. *J Clin Invest*, *120*, 93.

Kho, Y., Kim, S.C., Jiang, C., Barma, D., Kwon, S.W., Cheng, J., Jaunbergs, J., Weinbaum, C., Tamanoi, F., Falck, J., & Zhao, Y. (**2004**). A tagging-via-substrate technology for detection and proteomics of farnesylated proteins. *Proc Natl Acad Sci U S A*, *101*, 12479.

Kilroy, E.A., Ignacz, A.C., Brann, K.L., Schaffer, C.E., Varney, D., Alrowaished, S.S., Silknitter, K.J., Miner, J.N., Almaghasilah, A., Spellen, T.L., Lewis, A.D., Tilbury, K., King, B.L., Kelley, J.B., & Henry, C.A. (**2022**). Beneficial impacts of neuromuscular electrical stimulation on muscle structure and function in the zebrafish model of Duchenne muscular dystrophy. *Elife*, *11*, 62760.

Kim, D.H., Sarbassov, D.D., Ali, S.M., King, J.E., Latek, R.R., Erdjument-Bromage, H., Tempst, P., & Sabatini, D.M. (**2002**). mTOR interacts with raptor to form a nutrient-sensitive complex that signals to the cell growth machinery. *Cell*, *110*, 163–175.

Kim, D.H., Sarbassov, D.D., Ali, S.M., Latek, R.R., Guntur, K.V.P., Erdjument-Bromage, H., Tempst, P., & Sabatini, D.M. (**2003**). GβL, a positive regulator of the rapamycin-sensitive pathway required for the nutrient-sensitive interaction between raptor and mTOR. *Mol Cell*, *11*, 895–904.

Kimmel, C.B., Ballard, W.W., Kimmel, S.R., Ullmann, B., & Schilling, T.F. (**1995**). Stages of embryonic development of the zebrafish. *Dev Dyn*, *203*, 253–310.

Kodama, N., & Sekiguchi, S. (**1984**). The development of spontaneous body movement in prenatal and perinatal mice. *Dev Psychobiol*, *17*, 139–150.

Kou, X., Chen, D., & Chen, N. (**2019**). Physical activity alleviates cognitive dysfunction of alzheimer's disease through regulating the mTOR signaling pathway. *Int J Mol Sci*, *20*, 1591.

Lacher, M.D., Pincheira, R., Zhu, Z., Camoretti-Mercado, B., Matli, M., Warren, R.S., & Castro, A.F. (**2010**). Rheb activates AMPK and reduces p27Kip1 levels in Tsc2-null cells via mTORC1-independent mechanisms: implications for cell proliferation and tumorigenesis. *Oncogene*, *29*, 6543–6556.

Leduc-Gaudet, J.P., Franco-Romero, A., Cefis, M., Moamer, A., Broering, F.E., Milan, G., Sartori, R., Chaffer, T.J., Dulac, M., Marcangeli, V., Mayaki, D., Huck, L., Shams, A., Morais, J.A., Duchesne, E., Lochmuller, H., Sandri, M., Hussain, S.N.A., & Gouspillou, G. (**2023**). MYTHO is a novel regulator of skeletal muscle autophagy and integrity. *Nat Commun*, *14*, 1–20.

Lefebvre, A.K., Korneeva, N.L., Trutschl, M., Cvek, U., Duzan, R.D., Bradley, C.A., Hershey, J.W.B., & Rhoads, R.E. (**2006**). Translation initiation factor eIF4G-1 binds to eIF3 through the eIF3e subunit. *J Biol Chem*, *281*, 22917.

Lewis, J., Hanisch, A., & Holder, M. (**2009**). Notch signaling, the segmentation clock, and the patterning of vertebrate somites. *J Biol*, *8*, 44.

Li, Y., Inoki, K., & Guan, K.-L. (**2004**). Biochemical and functional characterizations of small GTPase Rheb and TSC2 GAP activity. *Mol Cell Biol*, *24*, 7965.

Liu, G.Y., & Sabatini, D.M. (**2020**). mTOR at the nexus of nutrition, growth, ageing and disease. *Nat Rev Mol Cell Biol*, *21*, 183.

Liu, L., Zhu, S., Gong, Z., & Low, B.C. (**2008**). K-ras/PI3K-Akt signaling Is essential for zebrafish hematopoiesis and angiogenesis. *PLoS One*, *3*, 2850.

Long, X., Lin, Y., Ortiz-Vega, S., Yonezawa, K., & Avruch, J. (**2005**). Rheb binds and regulates the mTOR kinase. *Curr Biol*, *15*, 702–713.

Ma, D., Bai, X., Guo, S., & Jiang, Y. (**2008**). The Switch I Region of Rheb is critical for its interaction with FKBP38. *J Biol Chem*, *283*, 25963.

Ma, L., Chen, Z., Erdjument-Bromage, H., Tempst, P., & Pandolfi, P.P. (**2005**). Phosphorylation and functional inactivation of TSC2 by Erk: implications for tuberous sclerosis and cancer pathogenesis. *Cell*, *121*, 179–193.

Ma, X.M., & Blenis, J. (**2009**). Molecular mechanisms of mTOR-mediated translational control. *Nat Rev Mol Cell Biol*, *10*, 307–318.

Marcotte, G.R., West, D.W.D., & Baar, K. (**2015**). The molecular basis for load-induced skeletal muscle hypertrophy. *Calcif Tissue Int*, *96*, 196.

Mayer, C., & Grummt, I. (**2006**). Ribosome biogenesis and cell growth: mTOR coordinates transcription by all three classes of nuclear RNA polymerases. *Oncogene*, *25*, 6384–6391.

Mayer, C., Zhao, J., Yuan, X., & Grummt, I. (**2004**). mTOR-dependent activation of the transcription factor TIF-IA links rRNA synthesis to nutrient availability. *Genes Dev*, *18*, 423.

Mazhab-Jafari, M.T., Marshall, C.B., Ishiyama, N., Ho, J., Di Palma, V., Stambolic, V., & Ikura, M. (**2012**). An autoinhibited noncanonical mechanism of GTP hydrolysis by Rheb maintains mTORC1 homeostasis. *Structure*, *20*, 1528–1539.

McGee, S.L., Howlett, K.F., Starkie, R.L., Cameron-Smith, D., Kemp, B.E., & Hargreaves, M. (**2003**). Exercise increases nuclear AMPK alpha2 in human skeletal muscle. *Diabetes*, *52*, 926–928.

Melser, S., Chatelain, E.H., Lavie, J., Mahfouf, W., Jose, C., Obre, E., Goorden, S., Priault, M., Elgersma, Y., Rezvani, H.R., Rossignol, R., & Bénard, G. (**2013**). Rheb regulates mitophagy induced by mitochondrial energetic status. *Cell Metab*, *17*, 719–730.

Meng, W., Liang, X., Xiao, T., Wang, J., Wen, J., Luo, H., Teng, J., Fei, Y., Zhang, Q., Liu, B., Hu, F., Bai, J., Liu, M., Zhou, Z., Liu, F., & Wu, J. (**2019**). Rheb promotes brown fat thermogenesis by Notch-dependent activation of the PKA signaling pathway. *J Mol Cell Biol*, *11*, 781.

Michels, A.A., Robitaille, A.M., Buczynski-Ruchonnet, D., Hodroj, W., Reina, J.H., Hall, M.N., & Hernandez, N. (**2010**). mTORC1 directly phosphorylates and regulates human MAF1. *Mol Cell Biol*, *30*, 3749.

Mommsen, T.P. (**2001**). Paradigms of growth in fish. *Comp Biochem Physiol B Biochem Mol Biol*, *129*, 207–219.

Mori, T., Ato, S., Knudsen, J.R., Henriquez-Olguin, C., Li, Z., Wakabayashi, K., Suginohara, T., Higashida, K., Tamura, Y., Nakazato, K., Jensen, T.E., & Ogasawara, R. (**2021**). c-Myc overexpression increases ribosome biogenesis and protein synthesis independent of mTORC1 activation in mouse skeletal muscle. *Am J Physiol Endocrinol Metab*, *321*, E551–E559.

Morita, M., Gravel, S.P., Chénard, V., Sikström, K., Zheng, L., Alain, T., Gandin, V., Avizonis, D., Arguello, M., Zakaria, C., McLaughlan, S., Nouet, Y., Pause, A., Pollak, M., Gottlieb, E., Larsson, O., St-Pierre, J., Topisirovic, I., & Sonenberg, N. (**2013**). mTORC1 controls mitochondrial activity and biogenesis through 4E-BP-dependent translational regulation. *Cell Metab*, *18*, 698–711.

Morita, M., Gravel, S.P., Hulea, L., Larsson, O., Pollak, M., St-Pierre, J., & Topisirovic, I. (**2015**). mTOR coordinates protein synthesis, mitochondrial activity and proliferation. *Cell Cycle*, *14*, 473.

Mounier, R., Lantier, L., Leclerc, J., Sotiropoulos, A., Pende, M., Daegelen, D., Sakamoto, K., Foretz, M., & Viollet, B. (**2009**). Important role for AMPKalpha1 in limiting skeletal muscle cell hypertrophy. *FASEB J*, *23*, 2264–2273.

Nakashima, K., & Yakabe, Y. (**2007**). AMPK activation stimulates myofibrillar protein degradation and expression of atrophy-related ubiquitin ligases by increasing FOXO

transcription factors in C2C12 myotubes. *Biosci Biotechnol Biochem*, *71*, 1650–1656.

Navaratnam, V., Kaufman, M.H., Skepper, J.N., Barton, S., & Guttridge, K.M. (**1986**). Differentiation of the myocardial rudiment of mouse embryos: an ultrastructural study including freeze-fracture replication. *J Anat*, *146*, 65–85.

Norizadeh Abbariki, T. (**2021**). Skeletal muscle plasticity: The LIM domain protein nTRIP6 in muscle regeneration, nuclear function of the mTORC1 activator RHEB in muscle growth (PhD Thesis). *Karlsruher Institut Für Technologie (KIT)*, 1–108.

Ogata, T., & Yamasaki, Y. (**1987**). High -resolution scanning electron-microscopic studies on the three-dimensional structure of mitochondria and sarcoplasmic reticulum in the different twitch muscle fibers of the frog. *Cell Tissue Res*, *250*, 489–497.

Oh, W.J., & Jacinto, E. (**2011**). mTOR complex 2 signaling and functions. *Cell Cycle*, *10*, 2305.

O'Neill, H.M., Maarbjerg, S.J., Crane, J.D., Jeppesen, J., Jørgensen, S.B., Schertzer, J.D., Shyroka, O., Kiens, B., Van Denderen, B.J., Tarnopolsky, M.A., Kemp, B.E., Richter, E.A., & Steinberg, G.R. (**2011**). AMP-activated protein kinase (AMPK) β1β2 muscle null mice reveal an essential role for AMPK in maintaining mitochondrial content and glucose uptake during exercise. *Proc Natl Acad Sci U S A*, *108*, 16092–16097.

Osaka, N., Hirota, Y., Ito, D., Ikeda, Y., Kamata, R., Fujii, Y., Chirasani, V.R., Campbell, S.L., Takeuchi, K., Senda, T., & Sasaki, A.T. (**2021**). Divergent mechanisms activating RAS and small GTPases through post-translational modification. *Front Mol Biosci*, *8*, 707439.

Palomero, T., Wei, K.L., Odom, D.T., Sulis, M.L., Real, P.J., Margolin, A., Barnes, K.C., O'Neil, J., Neuberg, D., Weng, A.P., Aster, J.C., Sigaux, F., Soulier, J., Look, A.T., Young, R.A., Califano, A., & Ferrando, A.A. (**2006**). NOTCH1 directly regulates c-

MYC and activates a feed-forward-loop transcriptional network promoting leukemic cell growth. *Proc Natl Acad Sci U S A*, *103*, 18261.

Palstra, A.P., Rovira, M., Rizo-Roca, D., Torrella, J.R., Spaink, H.P., & Planas, J. V. (**2014**). Swimming-induced exercise promotes hypertrophy and vascularization of fast skeletal muscle fibres and activation of myogenic and angiogenic transcriptional programs in adult zebrafish. *BMC Genomics*, *15*, 1136.

Palstra, A.P., Tudorache, C., Rovira, M., Brittijn, S.A., Burgerhout, E., van den Thillart, G.E.E.J.M., Spaink, H.P., & Planas, J. V. (**2010**). Establishing zebrafish as a novel exercise model: swimming economy, swimming-enhanced growth and muscle growth marker gene expression. *PLoS One*, *5*, e14483.

Panov, K.I., Friedrich, J.K., Russell, J., & Zomerdijk, J.C.B.M. (**2006**). UBF activates RNA polymerase I transcription by stimulating promoter escape. *EMBO J*, *25*, 3310.

Parmar, N., & Tamanoi, F. (**2010**). Rheb G-Proteins and the activation of mTORC1. *Enzymes*, *27*, 39.

Pelster, B., Sänger, A.M., Siegele, M., & Schwerte, T. (**2003**). Influence of swim training on cardiac activity, tissue capillarization, and mitochondrial density in muscle tissue of zebrafish larvae. *Am J Physiol Regul Integr Comp Physiol*, *285*, R339–R347.

Perl, A. (**2015**). mTOR activation is a biomarker and a central pathway to autoimmune disorders, cancer, obesity, and aging. *Ann N Y Acad Sci*, *1346*, 33.

Peterson, T.R., Sengupta, S.S., Harris, T.E., Carmack, A.E., Kang, S.A., Balderas, E., Guertin, D.A., Madden, K.L., Carpenter, A.E., Finck, B.N., & Sabatini, D.M. (**2011**). mTOR complex 1 regulates lipin 1 localization to control the SREBP pathway. *Cell*, *146*, 408.

Petkov, S., Brenmoehl, J., Langhammer, M., Hoeflich, A., & Röntgen, M. (**2022**). Myogenic precursor cells show faster activation and enhanced differentiation in a male mouse model selected for advanced endurance exercise performance. *Cells*, *11*, 1001.

Porstmann, T., Santos, C.R., Griffiths, B., Cully, M., Wu, M., Leevers, S., Griffiths, J.R., Chung, Y.L., & Schulze, A. (**2008**). SREBP activity Is regulated by mTORC1 and contributes to Akt-dependent cell growth. *Cell Metab*, *8*, 224.

Rabanal-Ruiz, Y., Otten, E.G., & Korolchuk, V.I. (**2017**). mTORC1 as the main gateway to autophagy. *Essays Biochem*, *61*, 565.

Rennie, M.J., Wackerhage, H., Spangenburg, E.E., & Booth, F.W. (**2004**). Control of the size of the human muscle mass. *Annu Rev Physiol*, *66*, 799–828.

Rescan, P.Y. (**2001**). Regulation and functions of myogenic regulatory factors in lower vertebrates. *Comp Biochem Physiol B Biochem Mol Biol*, *130*, 1–12.

Richardson, R., Tracey-White, D., Webster, A., & Moosajee, M. (**2017**). The zebrafish eye - a paradigm for investigating human ocular genetics. *Eye (Lond)*, *31*, 68–86.

Risson, V., Mazelin, L., Roceri, M., Sanchez, H., Moncollin, V., Corneloup, C., Richard-Bulteau, H., Vignaud, A., Baas, D., Defour, A., Freyssenet, D., Tanti, J.F., Le-Marchand-Brustel, Y., Ferrier, B., Conjard-Duplany, A., Romanino, K., Bauché, S., Hantaï, D., Mueller, M., … Gangloff, Y.G. (**2009**). Muscle inactivation of mTOR causes metabolic and dystrophin defects leading to severe myopathy. *J Cell Biol*, *187*, 859.

Rommel, C., Bodine, S.C., Clarke, B.A., Rossman, R., Nunez, L., Stitt, T.N., Yancopoulos, G.D., & Glass, D.J. (**2001**). Mediation of IGF-1-induced skeletal myotube hypertrophy by PI(3)K/Akt/mTOR and PI(3)K/Akt/GSK3 pathways. *Nat Cell Biol*, *3*, 1009–1013.

Rowlerson, A., & Veggetti, A. (**2001**). Cellular mechanisms of post-embryonic muscle growth in aquaculture species. *Fish Physiology*, *18*, 103–140.

Saga, Y. (**2012**). The mechanism of somite formation in mice. *Curr Opin Genet Dev*, *22*, 331–338.

Saint-Amant, L., & Drapeau, P. (**1998**). Time course of the development of motor behaviors in the zebrafish embryo. *J Neurobiol*, *37*, 622–632.

Sancak, Y., Bar-Peled, L., Zoncu, R., Markhard, A.L., Nada, S., & Sabatini, D.M. (**2010**). Ragulator-Rag complex targets mTORC1 to the lysosomal surface and is necessary for its activation by amino acids. *Cell*, *141*, 290.

Sancak, Y., Peterson, T.R., Shaul, Y.D., Lindquist, R.A., Thoreen, C.C., Bar-Peled, L., & Sabatini, D.M. (**2008**). The Rag GTPases bind raptor and mediate amino acid signaling to mTORC1. *Science*, *320*, 1496.

Sanchez, A.M.J., Csibi, A., Raibon, A., Cornille, K., Gay, S., Bernardi, H., & Candau, R. (**2012**). AMPK promotes skeletal muscle autophagy through activation of forkhead FoxO3a and interaction with Ulk1. *J Cell Biochem*, *113*, 695–710.

Sandri, M. (**2008**). Signaling in muscle atrophy and hypertrophy. *Physiology*, *23*, 160–170.

Sato, T., Akasu, H., Shimono, W., Matsu, C., Fujiwara, Y., Shibagaki, Y., Heard, J.J., Tamanoi, F., & Hattori, S. (**2015**). Rheb protein binds CAD (Carbamoyl-phosphate Synthetase 2, Aspartate Transcarbamoylase, and Dihydroorotase) protein in a GTP- and effector domain-dependent manner and influences its cellular localization and carbamoyl-phosphate synthetase (CPSase) activity. *J Biol Chem*, *290*, 1096.

Sato, T., Nakashima, A., Guo, L., & Tamanoi, F. (**2009**). Specific activation of mTORC1 by Rheb G-protein in vitro involves enhanced recruitment of its substrate protein. *J Biol Chem*, *284*, 12783.

Schalm, S.S., & Blenis, J. (**2002**). Identification of a conserved motif required for mTOR signaling. *Curr Biol*, *12*, 632–639.

Schiaffino, S., & Mammucari, C. (**2011**). Regulation of skeletal muscle growth by the IGF1-Akt/PKB pathway: insights from genetic models. *Skelet Muscle*, *1*, 4.

Schindelin, J., Arganda-Carreras, I., Frise, E., Kaynig, V., Longair, M., Pietzsch, T., Preibisch, S., Rueden, C., Saalfeld, S., Schmid, B., Tinevez, J.Y., White, D.J., Hartenstein, V., Eliceiri, K., Tomancak, P., & Cardona, A. (**2012**). Fiji: an open-source platform for biological-image analysis. *Nat Methods*, *9*, 676–682.

Seger, C., Hargrave, M., Wang, X., Chai, R.J., Elworthy, S., & Ingham, P.W. (**2011**). Analysis of Pax7 expressing myogenic cells in zebrafish muscle development, injury, and models of disease. *Dev Dyn*, *240*, 2440–2451.

Sengupta, S., Peterson, T.R., & Sabatini, D.M. (**2010**). Regulation of the mTOR complex 1 pathway by nutrients, growth factors, and stress. *Mol Cell*, *40*, 310–322.

Steen, M.S., Adams, M.E., Tesch, Y., & Froehner, S.C. (**2009**). Amelioration of muscular dystrophy by transgenic expression of Niemann-Pick C1. *Mol Biol Cell*, *20*, 146.

Stellabotte, F., & Devoto, S.H. (**2007**). The teleost dermomyotome. *Dev Dyn*, *236*, 2432–2443.

Stellabotte, F., Dobbs-McAuliffe, B., Fernández, D.A., Feng, X., & Devoto, S.H. (**2007**). Dynamic somite cell rearrangements lead to distinct waves of myotome growth. *Development*, *134*, 1253–1257.

Stickney, H.L., Barresi, M.J.F., & Devoto, S.H. (**2000**). Somite development in zebrafish. *Dev Dyn*, *219*, 287–303.

Sugiura, H., Shimada, T., Moriya-Ito, K., Goto, J.I., Fujiwara, H., Ishii, R., Shitara, H., Taya, C., Fujii, S., Kobayashi, T., Hino, O., Worley, P.F., & Yamagata, K. (**2022**). A farnesyltransferase inhibitor restores cognitive deficits in Tsc2+/– mice through inhibition of Rheb1. *J Neurosci*, *42*, 2598–2612.

Suzue, T. (**1996**). Movements of mouse fetuses in early stages of neural development studied in vitro. *Neurosci Lett*, *218*, 131–134.

Swinburne, I.A., Mosaliganti, K.R., Green, A.A., & Megason, S.G. (**2015**). Improved long-term imaging of embryos with genetically encoded α-Bungarotoxin. *PLoS One*, *10*, e0134005.

Tabancay, A.P., Gau, C.L., Machado, I.M.P., Uhlmann, E.J., Gutmann, D.H., Guo, L., & Tamanoi, F. (**2003**). Identification of dominant negative mutants of Rheb GTPase and their use to implicate the involvement of human Rheb in the activation of p70S6K. *J Biol Chem*, *278*, 39921–39930.

Takahashi, K., Nakagawa, M., Young, S.G., & Yamanaka, S. (**2005**). Differential membrane localization of ERas and Rheb, two Ras-related proteins involved in the phosphatidylinositol 3-kinase/mTOR pathway. *J Biol Chem*, *280*, 32768–32774.

Terzis, G., Georgiadis, G., Stratakos, G., Vogiatzis, I., Kavouras, S., Manta, P., Mascher, H., & Blomstrand, E. (**2008**). Resistance exercise-induced increase in muscle mass correlates with p70S6 kinase phosphorylation in human subjects. *Eur J Appl Physiol*, *102*, 145–152.

Tsang, C.K., Liu, H., & Zheng, X.F.S. (**2010**). mTOR binds to the promoters of RNA polymerase I- and III-transcribed genes. *Cell Cycle*, *9*, 953.

Tzartos, S.J., & Changeux, J.P. (**1983**). High affinity binding of alpha-bungarotoxin to the purified alpha-subunit and to its 27,000-dalton proteolytic peptide from Torpedo marmorata acetylcholine receptor. Requirement for sodium dodecyl sulfate. *EMBO J*, *2*, 381.

Uhlenbrock, K., Weiwad, M., Wetzker, R., Fischer, G., Wittinghofer, A., & Rubio, I. (**2009**). Reassessment of the role of FKBP38 in the Rheb/mTORC1 pathway. *FEBS Lett*, *583*, 965–970.

Veal, E.A., & Jackson, M.J. (**1998**). C-myc is expressed in mouse skeletal muscle nuclei during post-natal maturation. *Int J Biochem Cell Biol*, *30*, 811–821.

von Walden, F., Liu, C., Aurigemma, N., & Nader, G.A. (**2016**). mTOR signaling regulates myotube hypertrophy by modulating protein synthesis, rDNA transcription, and chromatin remodeling. *Am J Physiol Cell Physiol*, *311*, C663–C672.

Walker, S.M., & Edge, M.B. (**1971**). The sarcoplasmic reticulum and development of z lines in skeletal muscle fibers of fetal and postnatal rats. *Anat Rec*, *169*, 661–677.

Wang, X., & Proud, C.G. (**2006**). The mTOR pathway in the control of protein synthesis. *Physiology*, *21*, 362–369.

Waterman, R.E. (**1969**). Development of the lateral musculature in the teleost, Brachydanio rerio: a fine structural study. *Am J Anat*, *125*, 457–493.

Wen, Y., Alimov, A.P., & McCarthy, J.J. (**2016**). Ribosome biogenesis is necessary for skeletal muscle hypertrophy. *Exerc Sport Sci Rev*, *44*, 110.

Whyte, D.B., Kirschmeier, P., Hockenberry, T.N., Nunez-Oliva, I., James, L., Catino, J.J., Bishop, W.R., & Pai, J.K. (**1997**). K- and N-Ras are geranylgeranylated in cells treated with farnesyl protein transferase inhibitors. *J Biol Chem*, *272*, 14459–14464.

Williamson, D.L., Butler, D.C., & Alway, S.E. (**2009**). AMPK inhibits myoblast differentiation through a PGC-1α-dependent mechanism. *Am J Physiol Endocrinol Metab*, *297*, E304.

Xiao, Y., Ma, C., Yi, J., Wu, S., Luo, G., Xu, X., Lin, P.H., Sun, J., & Zhou, J. (**2015**). Suppressed autophagy flux in skeletal muscle of an amyotrophic lateral sclerosis mouse model during disease progression. *Physiol Rep*, *3*, e12271.

Yadav, R.B., Burgos, P., Parker, A.W., Iadevaia, V., Proud, C.G., Allen, R.A., O'Connell, J.P., Jeshtadi, A., Stubbs, C.D., & Botchway, S.W. (**2013**). mTOR direct interactions with Rheb-GTPase and raptor: sub-cellular localization using fluorescence lifetime imaging. *BMC Cell Biol*, *14*, 3.

Yamagata, K., Sanders, L.K., Kaufmann, W.E., Yee, W., Barnes, C.A., Nathans, D., & Worley, P.F. (**1994**). rheb, a growth factor- and synaptic activity-regulated gene, encodes a novel Ras-related protein. *J Biol Chem*, *269*, 16333–16339.

Yang, Q., Inoki, K., Kim, E., & Guan, K.L. (**2006**). TSC1/TSC2 and Rheb have different effects on TORC1 and TORC2 activity. *Proc Natl Acad Sci U S A*, *103*, 6811.

Yang, W., Pang, D., Chen, M., Wei, Y., Worley, P.F., Correspondence, B.X., & Edu, P. (**2021**). Rheb mediates neuronal-activity-induced mitochondrial energetics through mTORC1-independent PDH activation. *Dev Cell*, 811-825.e6.

Yin, H., Price, F., & Rudnicki, M.A. (**2013**). Satellite cells and the muscle stem cell niche. *Physiol Rev*, *93*, 23.

Yoon, M.S. (**2017**). mTOR as a key regulator in maintaining skeletal muscle mass. *Front Physiol*, *8*, 294538.

You, J.S., Mcnally, R.M., Jacobs, B.L., Privett, R.E., Gundermann, D.M., Lin, K.H., Steinert, N.D., Goodman, C.A., & Hornberger, T.A. (**2019**). The role of raptor in the mechanical load-induced regulation of mTOR signaling, protein synthesis, and skeletal muscle hypertrophy. *FASEB J*, *33*, 4021–4034.

Zhong, Y., Zhou, X., Guan, K.L., & Zhang, J. (**2022**). Rheb regulates nuclear mTORC1 activity independent of farnesylation. *Cell Chem Biol*, *29*, 1037-1045.e4.

Zhou, X., Clister, T.L., Lowry, P.R., Seldin, M.M., Wong, G.W., & Zhang, J. (**2015**). Dynamic visualization of mTORC1 activity in living cells. *Cell Rep*, *10*, 1767.

Zhou, Y., & Hancock, J.F. (**2018**). Deciphering lipid codes: K-Ras as a paradigm. *Traffic*, *19*, 157.

Zong, H., Ren, J.M., Young, L.H., Pypaert, M., Mu, J., Birnbaum, M.J., & Shulman, G.I. (**2002**). AMP kinase is required for mitochondrial biogenesis in skeletal muscle in response to chronic energy deprivation. *Proc Natl Acad Sci U S A*, *99*, 15983–15987.

6. Acknowledgements

Firstly, I sincerely thank Dr. Olivier Kassel for providing the opportunity to work in his laboratory and group on this truly exciting project. He was persistently an inspiring supervisor during my time in the lab.

Also, I am grateful to the other current and former members of the lab, whom I had the privilege to work with. Marga Litfin, who taught me so much during the initial phase of my PhD journey, was knowledgeable and helpful and with whom I had many great discussions.

Zita Gonda who started her PhD at the same time as I did and who was always helpful and insightful, especially as we faced similar challenges. Dr. Tannaz Norizadeh Abbariki, whose project I continued and who was a very supportive teacher during the beginning of my PhD. Dr. Christelle Etard, joining the lab partway through my time there, was a great addition to the team and incredibly helpful, particularly in working with Zebrafish.

I thank Dr. Felix Loosli and the members of his lab for not only providing the medaka embryos but also providing a tremendous amount of help in working with them. I thank the members of my TAC, Prof. Dr. Andrew Cato, Prof. Dr. Nicholas Foulkes, Jun-Prof. Dr. Lennart Hilbert and, of course, Dr Olivier Kassel, who helped me keep sight of my goals as well as helping me navigate several hurdles. Finally, I am grateful for my family and friends, who supported me during this time, especially my parents who kept me encouraged, especially in stressful periods.

Publications

Fettig, R., Gonda, Z., Walter, N., Sallmann, P., Thanisch, C., Winter, M., Bauer, S., Zhang, L., Linden, G., Litfin, M., Etard, C., Armant, O., Vázquez, O., & Kassel, O. (**2023**). Short internal open reading frames regulate the translation of N-terminally truncated proteoforms. *BioRxiv*, 2023.11.09.566418.